Coherent X-ray Imaging
Advanced Light Source, BL 9.0.1

ADVANCED LIGHT SOURCE
EXPERIMENTAL SYSTEMS GROUP

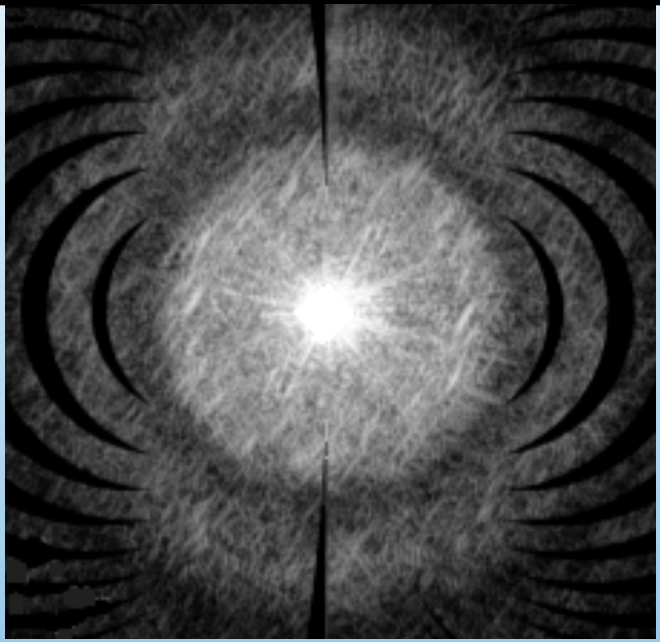

Motivation

- Obtain high resolution structural information about biological and material science specimens
- Develop experimental techniques optimized for upcoming coherent X-ray lasers

Beamline 9.0.1

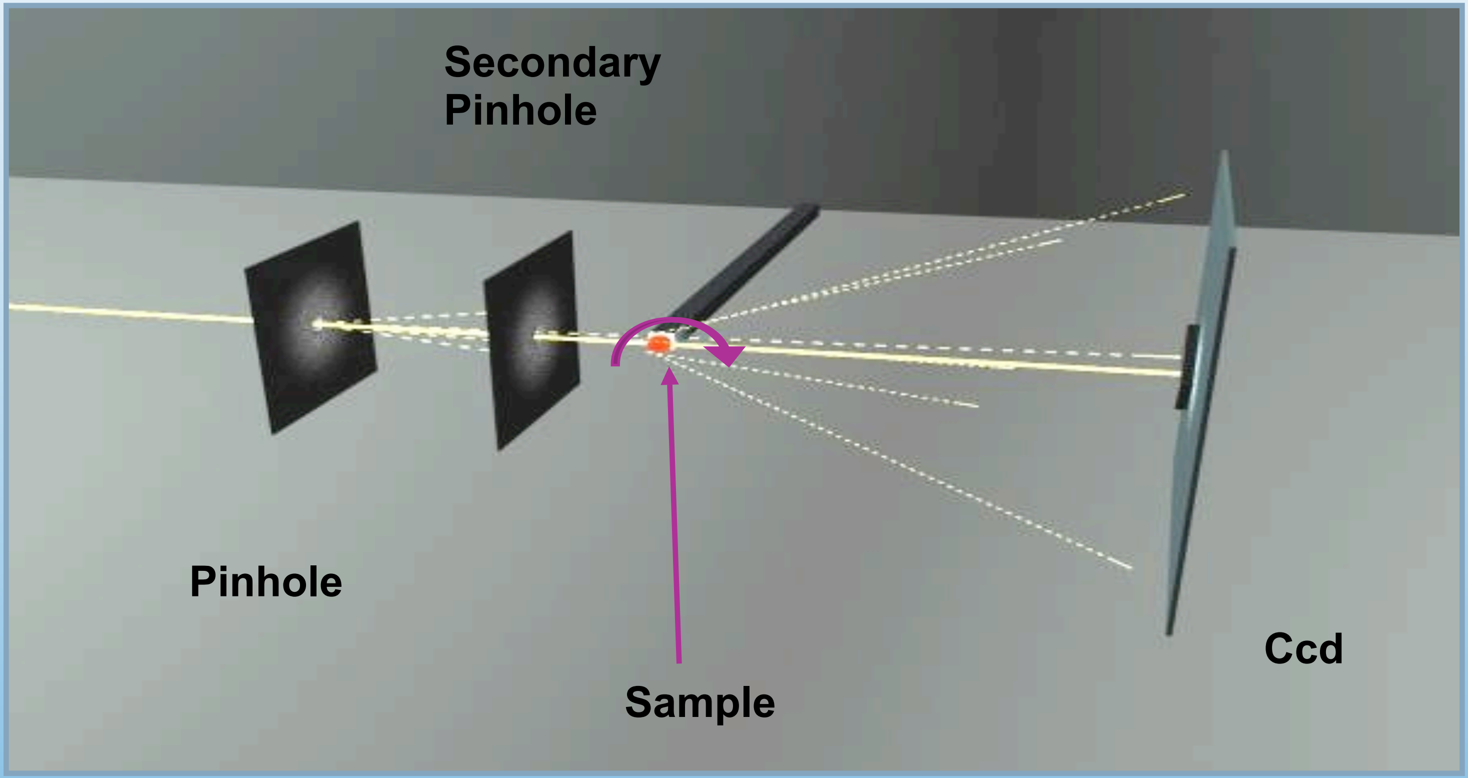

- A pinhole selects a monochromatic coherent x-ray beam
- A secondary pinhole cleans the beam
- X-rays: 520-750 eV (1500 eV upgrade in progress)
- Sample can be rotated perpendicular to x-rays
- Area detector collects the diffraction pattern *intensity*

Diffractive Imaging

Diffractive imaging is a form of microscopy whereby a lens is replaced by an array detector and a computer. The computer recovers the phases missing in the recorded intensity patterns.

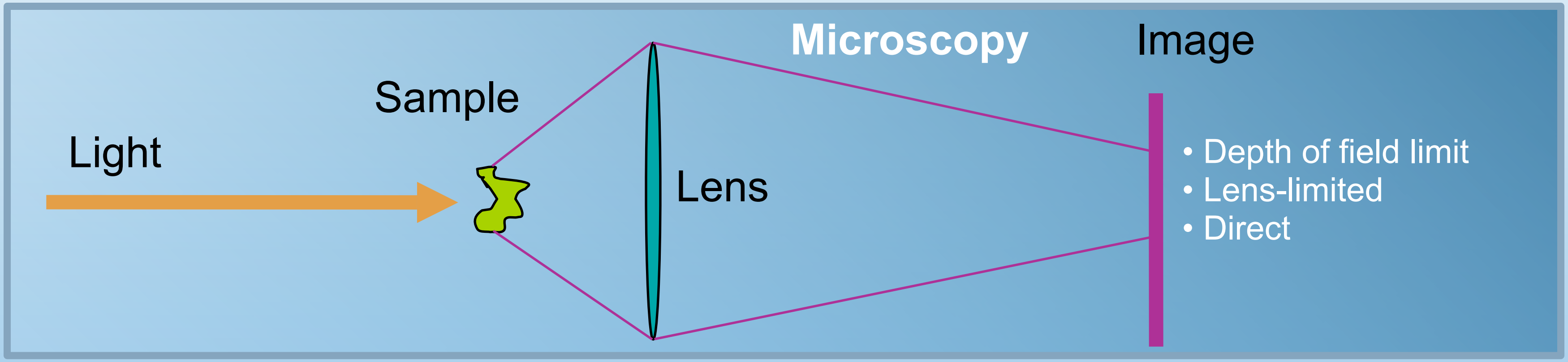

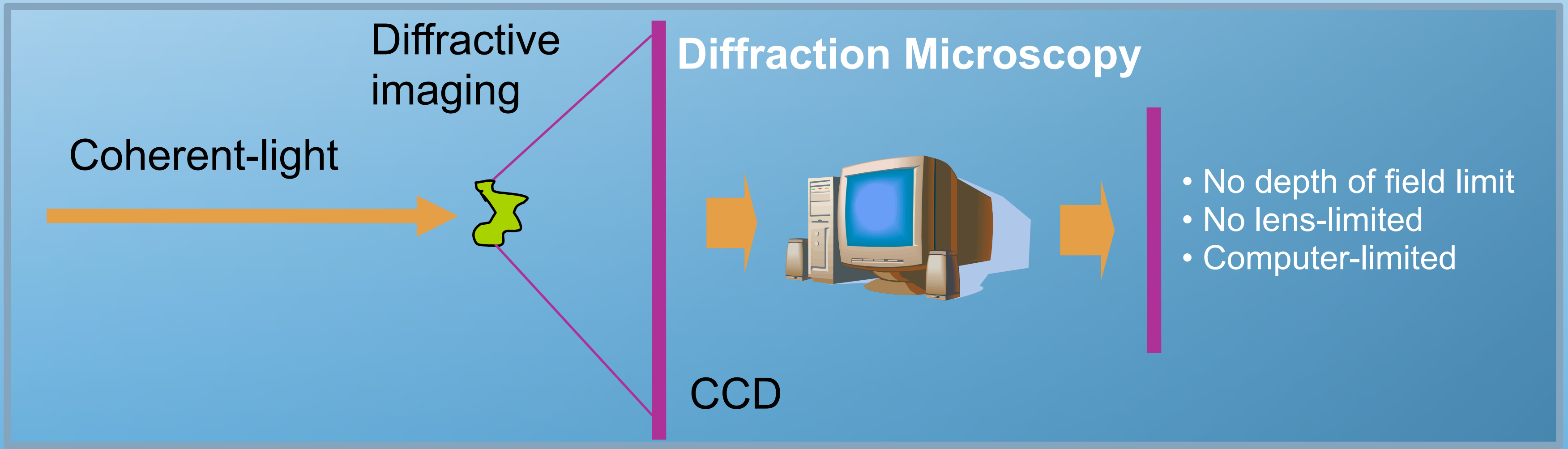

Proposed by D. Sayre, first demonstrated by J. Miao et al, in 1999

Overview Slide: Diffractive Imaging

Experimental

We can collect diffraction patterns at many orientations at the Advanced Light Source (wavelength: 1.6 nm)

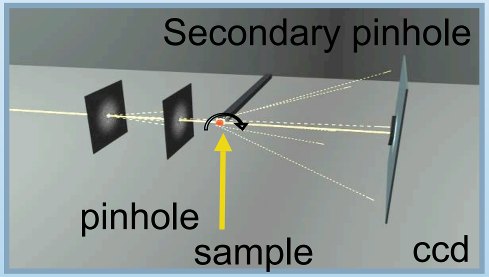

We solve the phase problem For 10^8 reflections

Stony Brook developed endstation for cryo imaging

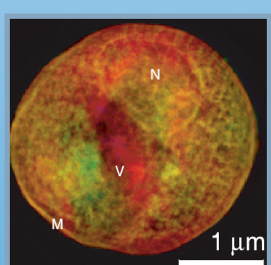

Yeast cell imaged at 40 nm resolution, D.Shapiro et al., *Proc. Nat. Acc. Sci. U.S.A.* 102, 15343-15346, (2005).

Click for more

Test object imaged in 3D

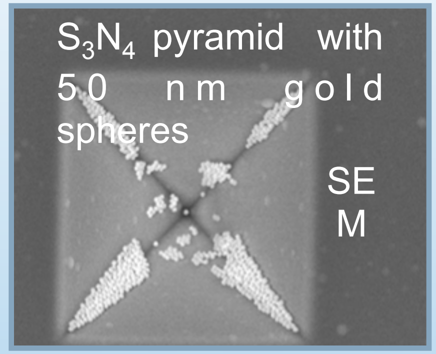

2D view

Algorithms

Shrinkwrap algorithm, S. Marchesini et al, Phys Rev B 68, 140101(R) (2003)

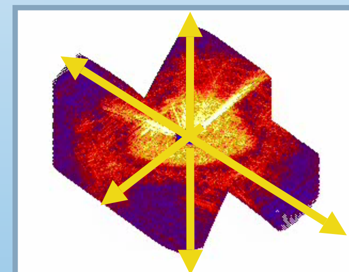

Chapman et al. J. Opt. Soc. Am A 23, 1179 (2006)

View

Ta_2O_5 Nanofoam

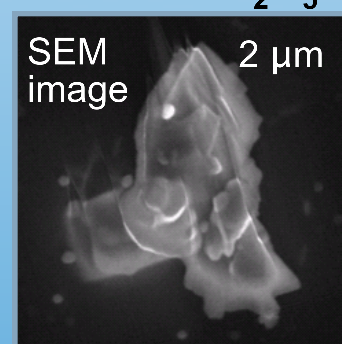

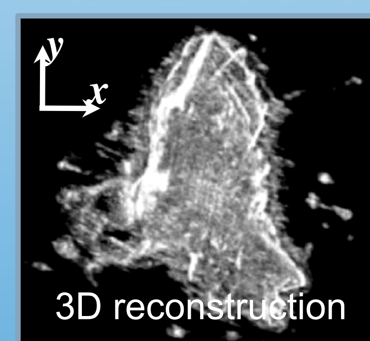

Structural properties of Aerogels revealed. Barty et al. submitted

View

Diffractive Imaging of Yeast cells

Motivation: obtain high resolution 3D images of cells

Gatan 630 cryo holder keeps cells frozen

Yeast cell: 2.5 micron thick,
unstained freeze-dried, at 750 eV
Total dose ~ 10^8 Gray (room temperature)
Oversampling is about 5 in each dimension

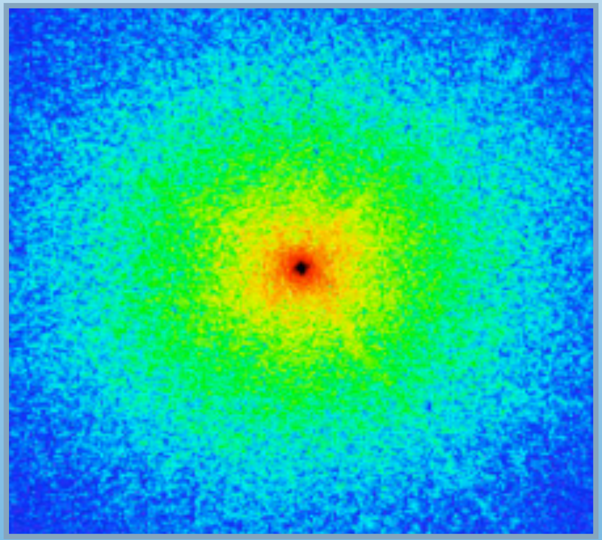

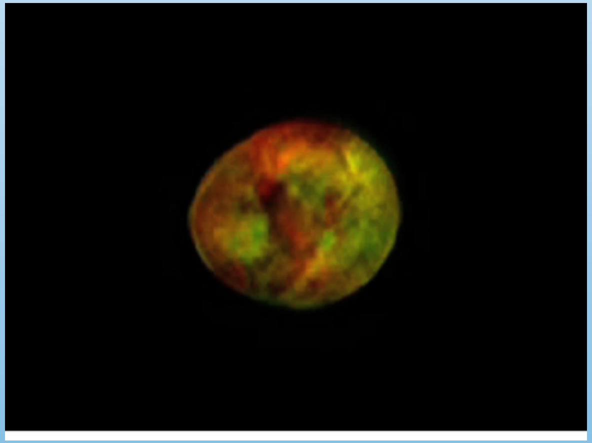

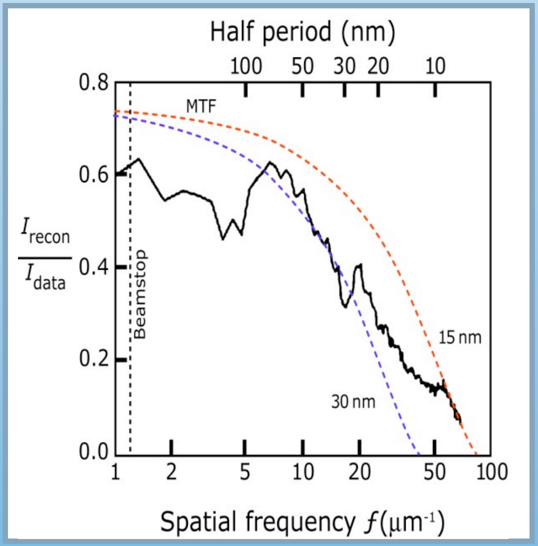

David Shapiro, Stony Brook, now at ALS

Consistency of reconstructions quantifies the resolution: 30 nm.

C. J. Jacobsen, J. Kirz, D. Shapiro et al.

3D Diffraction-imaging

- Complete coverage of reciprocal space by sample rotation
- Use a true 3D object that can be well-characterized by independent means

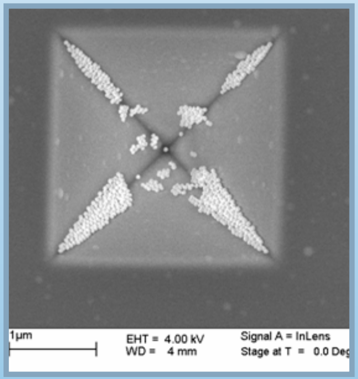

Diffraction patterns collected at multiple orientations

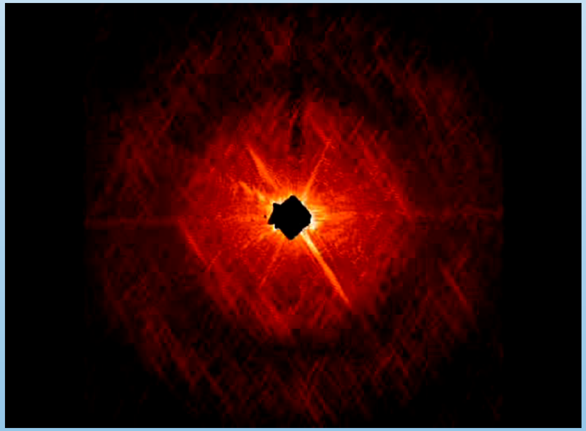

FFT

Autocorrelation obtained at multiple orientations

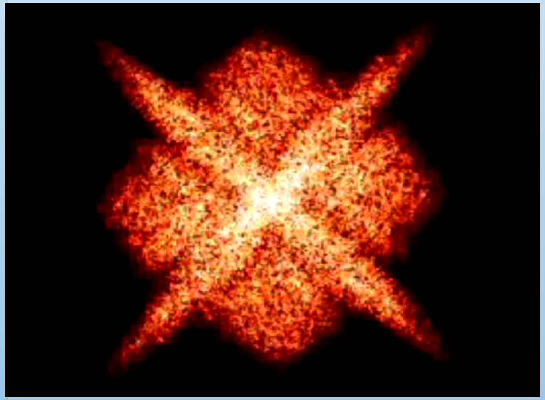

Multiple views (movie)

±70° range
1° angular spacing

3D Reconstruction Is Achieved by Fourier Synthesis

One diffraction pattern gives information on the Ewald sphere in reciprocal space

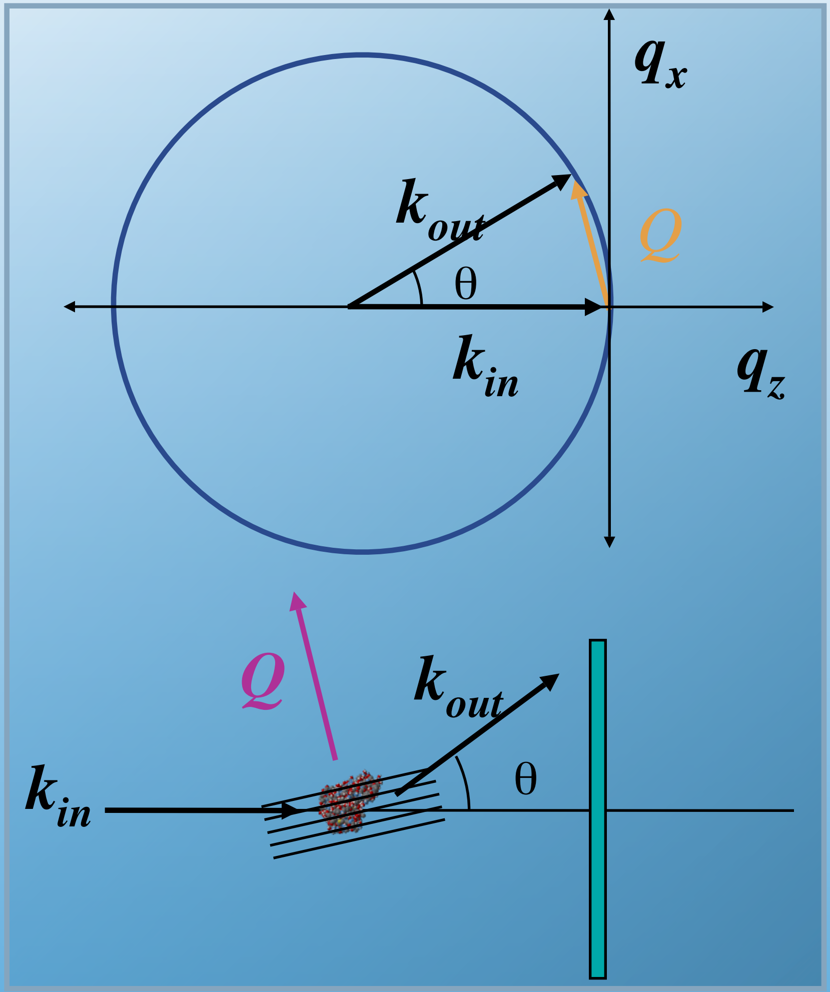

Rotating a sample about one axis allows to fill the data in Fourier space

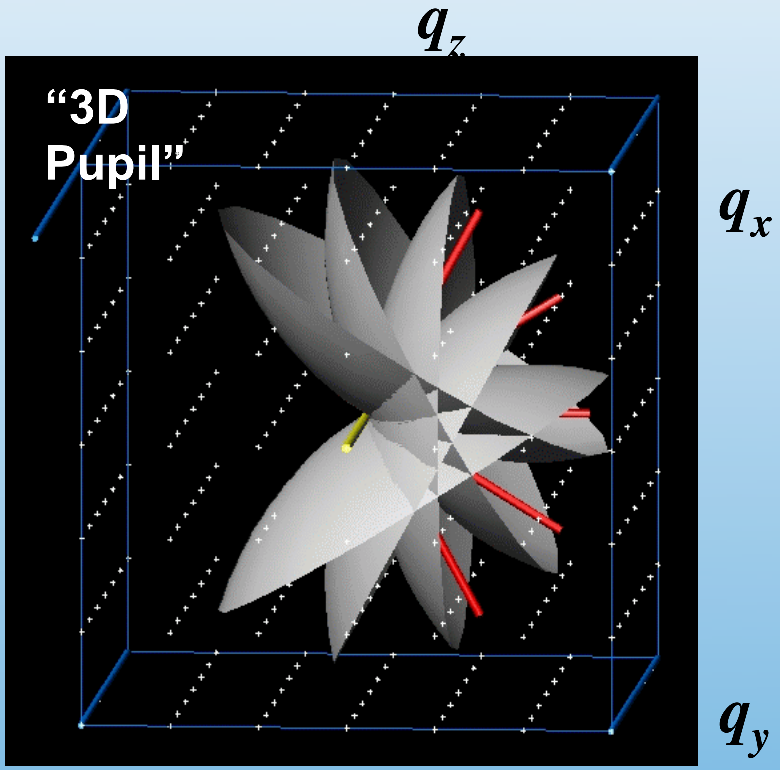

Full 3D Image Reconstructions From Experimental X-ray Data

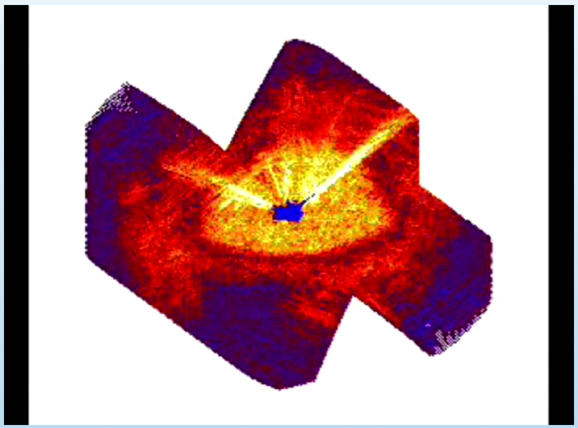

Voxel Data cube 1024^3 elements

Iterative reconstruction algorithm
1000s of 3D FFTs required

A. Barty

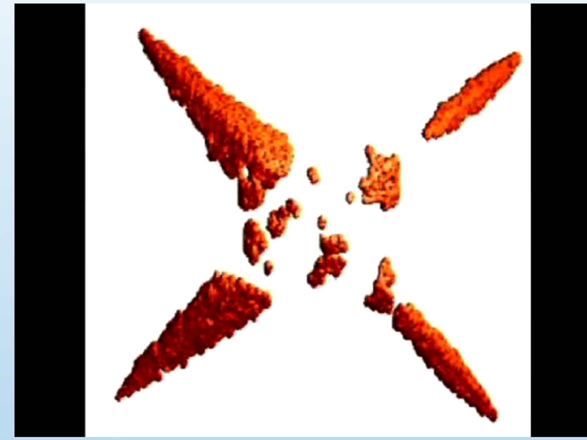

Reconstruction

Chapman et al. JOSAA 23, 1179 (2006)

Size	**Memory needed**	
	Single Precision	Double Precision
2563	336 MB	592 MB
5123	2.6 GB	4.7 Gb
10243	22 GB	38 GB
20483	176 GB	304 GB

Size	**32-CPU G5 cluster speed**	
	3D FFT timing	Processing time*
2563	73 msec	10 mins
5123	850 msec	1.5 hrs
10243	7.9 sec	14 hrs
20483	??	??

*2000 iterations, 2FFTs per iteration plus other floating point operations code: C with mvapich, dist_fft (Altivec-optimized MPI FFT) see http://images.apple.com/acg/pdf/20040827_GigaFFT.pdf

2D Single-view Images Have Depth Information

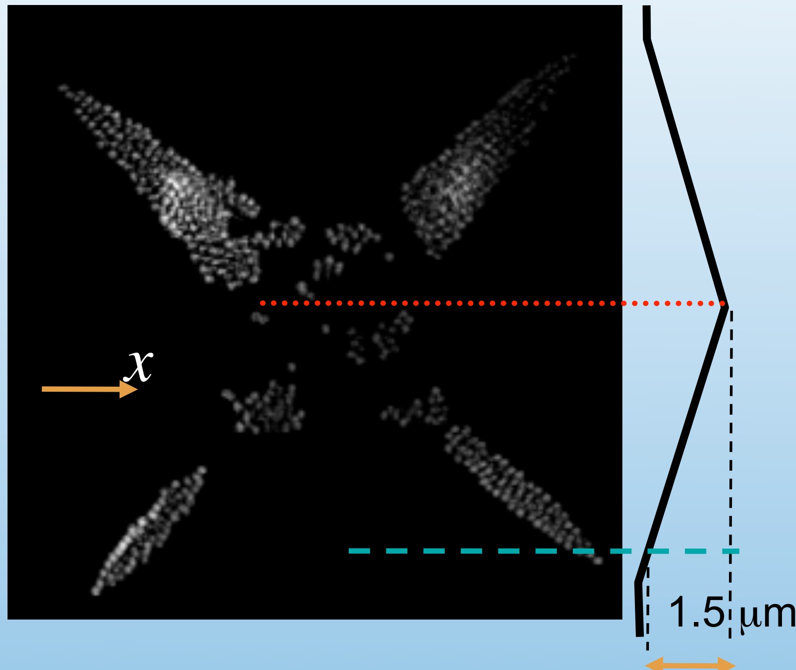

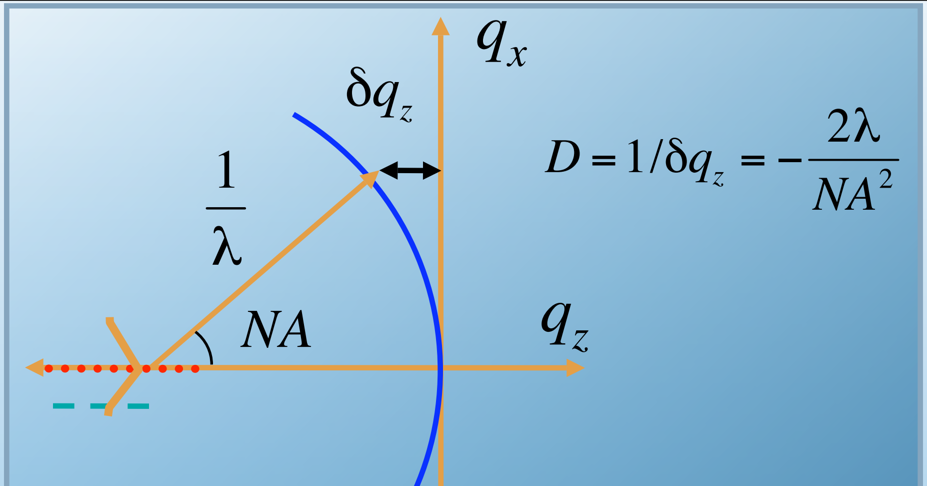

Images of objects thicker than D will differ from the projection image

Propagation of wavefield

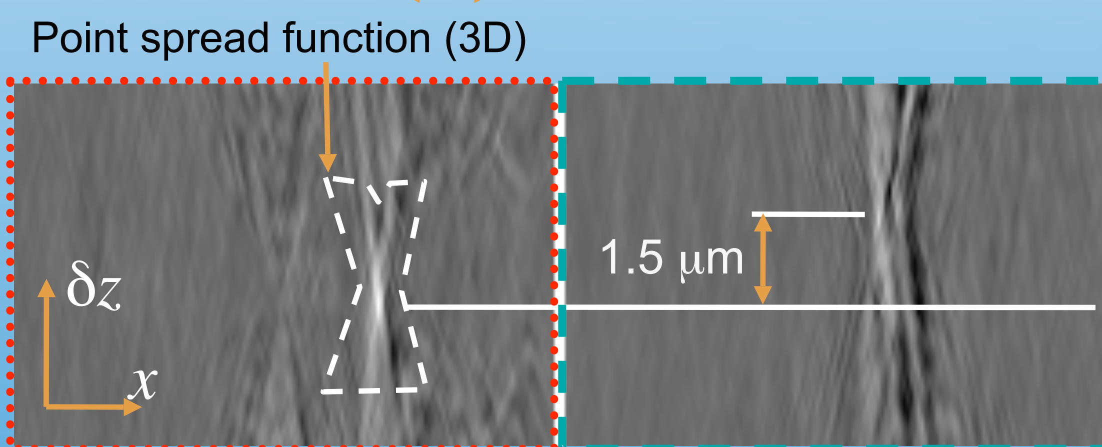

True 2D Projection Images Is Formed From a Central Section of the 3D Diffraction Data

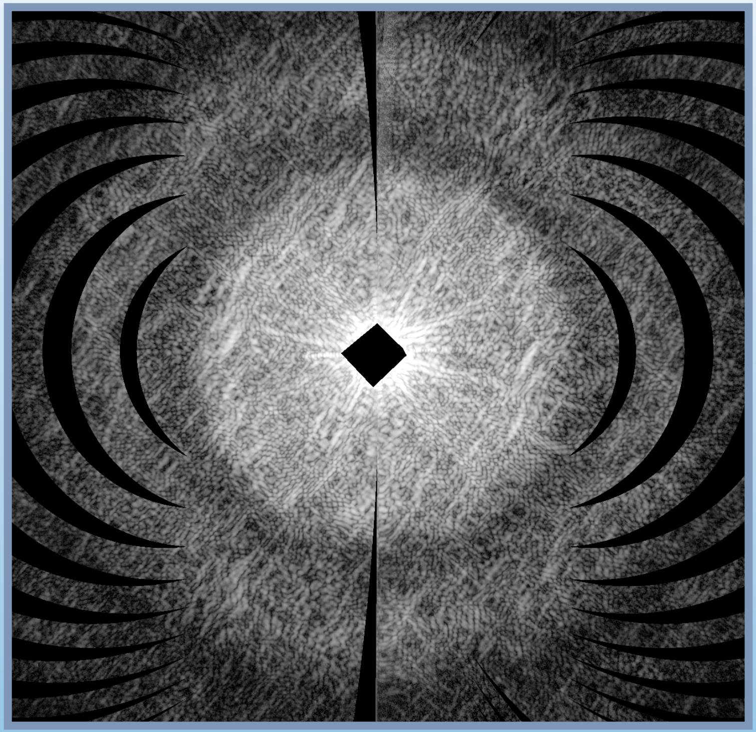

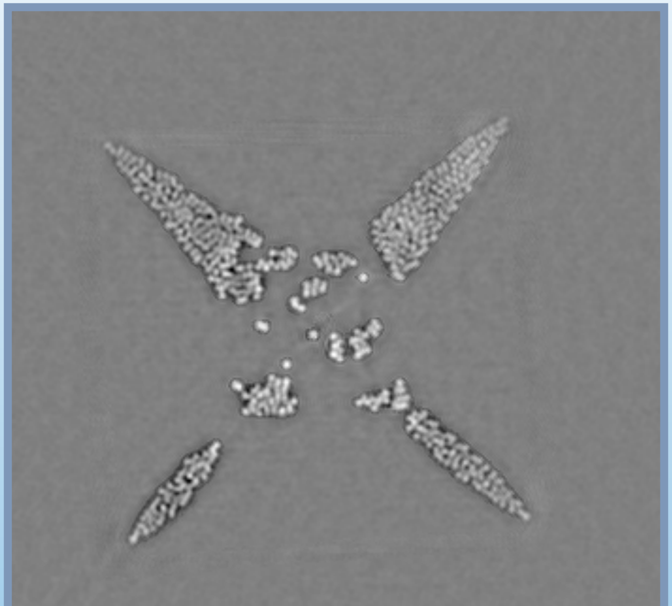

Infinite depth of focus

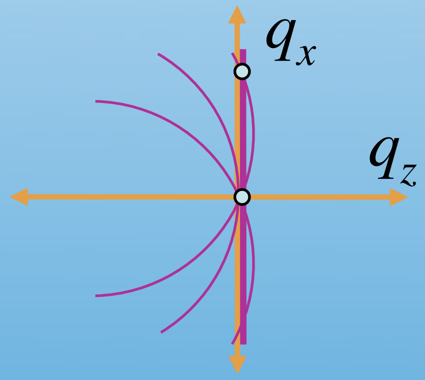

A true projection image is obtained from a **plane central section** of the 3D diffraction data. Data must be collected at many object orientations to achieve this

Coherent X-ray Diffraction Imaging of Aerogel Structures Compared With USAXS and TEM

Method	Rods radius (nm)	Rods length (nm)	Isotropic?
Diffraction Image	<13.7	44	no
USAXS	6.8	40	no ?
TEM	3-6	10-40	Can't be determined

Motivation
Aerogel strength/weight ratio depends on structural properties. We find a structure formed of blobs and rods, indicating pathways to make stronger and lighter materials

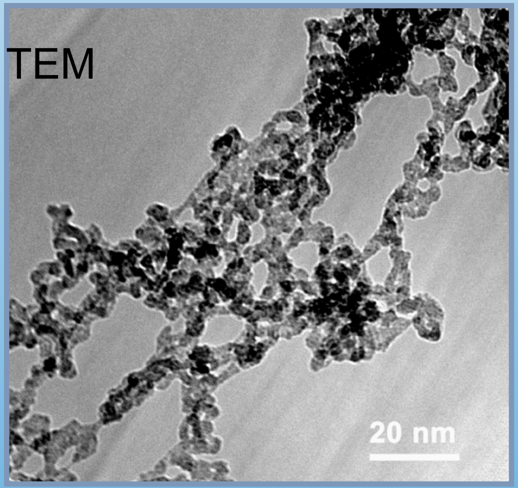

M. Wang (LLNL)

TEM results based on survey of 3-4 cells;
Diffraction based on ~300 cells.

USAXS

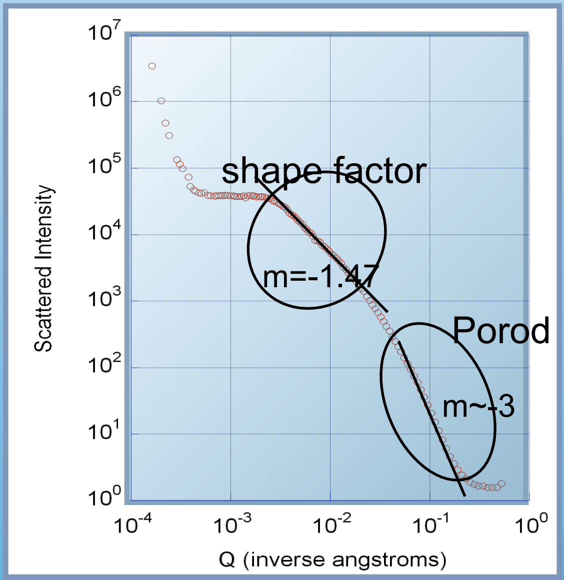

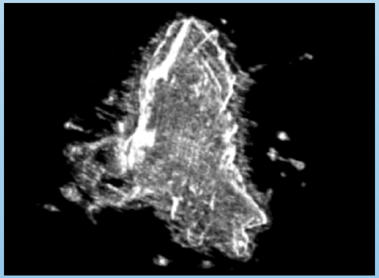

A. Barty (LLNL), submitted

Ultrafast Coherent Diffractive Imaging

Motivation: To study ultrafast dynamics and overcome radiation damage
We applied the techniques developed at ALS at the first X-FEL source

ALS, λ=1.6 nm

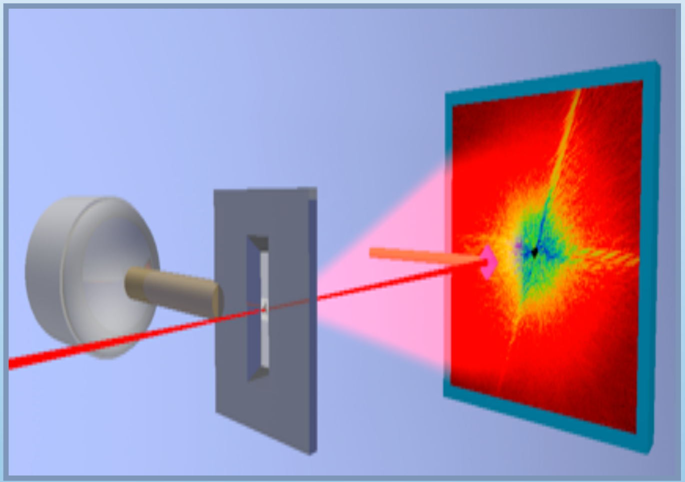

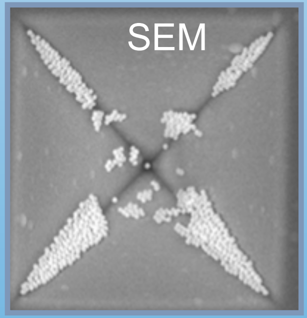

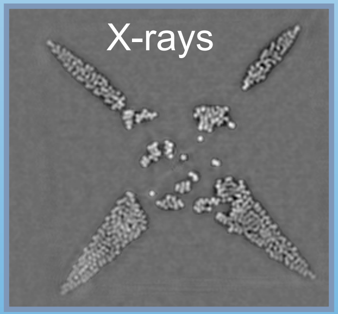

Chapman et al. JOSAA 23, 1179 (2006)

FLASH, λ=32 nm

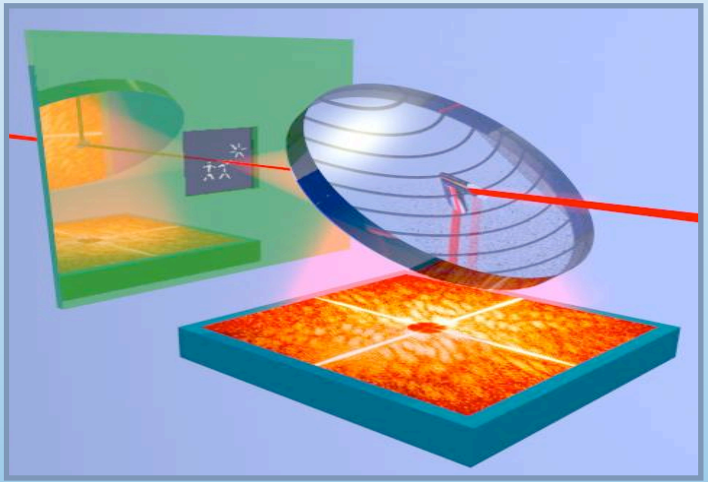

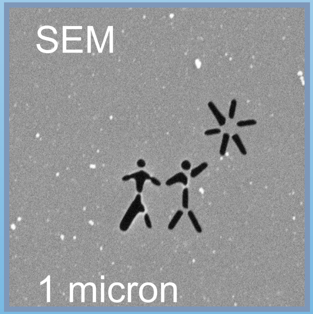

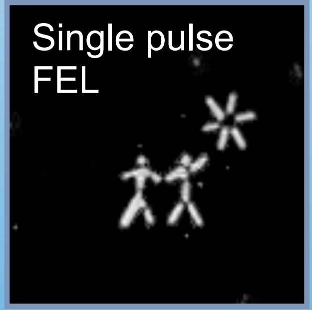

Chapman Et Al. Nature Physics 2, 839 - 843 (2006)

Image Reconstructed From an Ultrafast FEL Diffraction Pattern

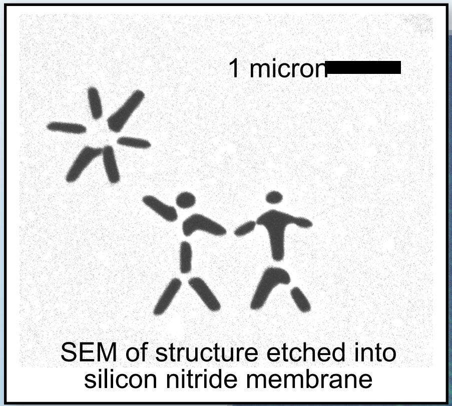

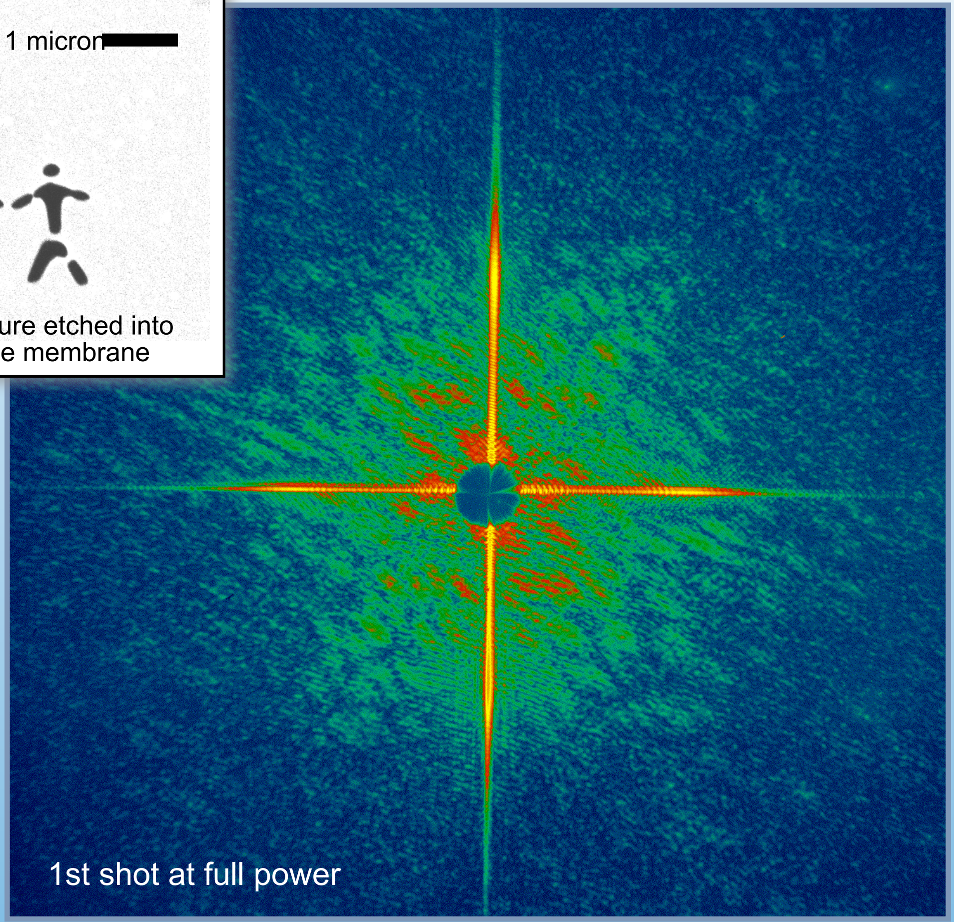

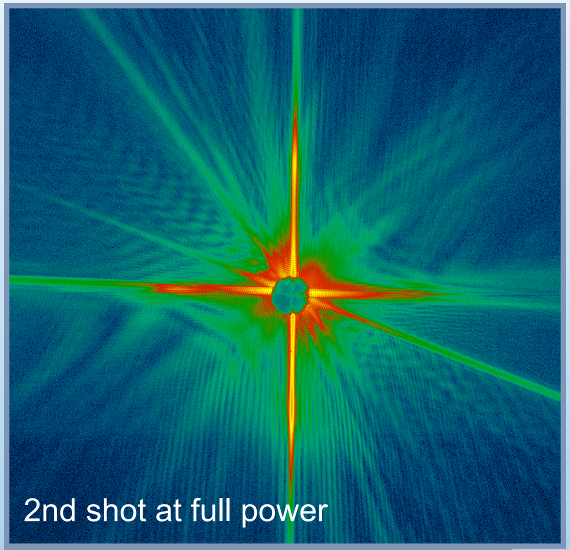

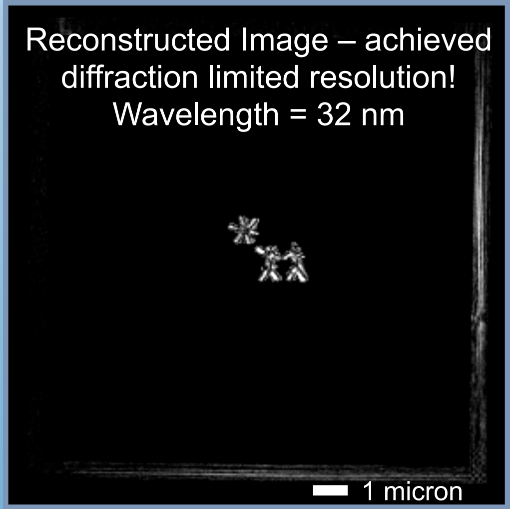

NA = 0.26. This is the highest numerical aperture coherent X-ray diffracton pattern ever reconstructed. Pixel size is 60 nm.

Chapman et al. Nature Physics 2, 839 - 843 (2006)

Overview Slide: Massively Parallel Holography With Coded Apertures

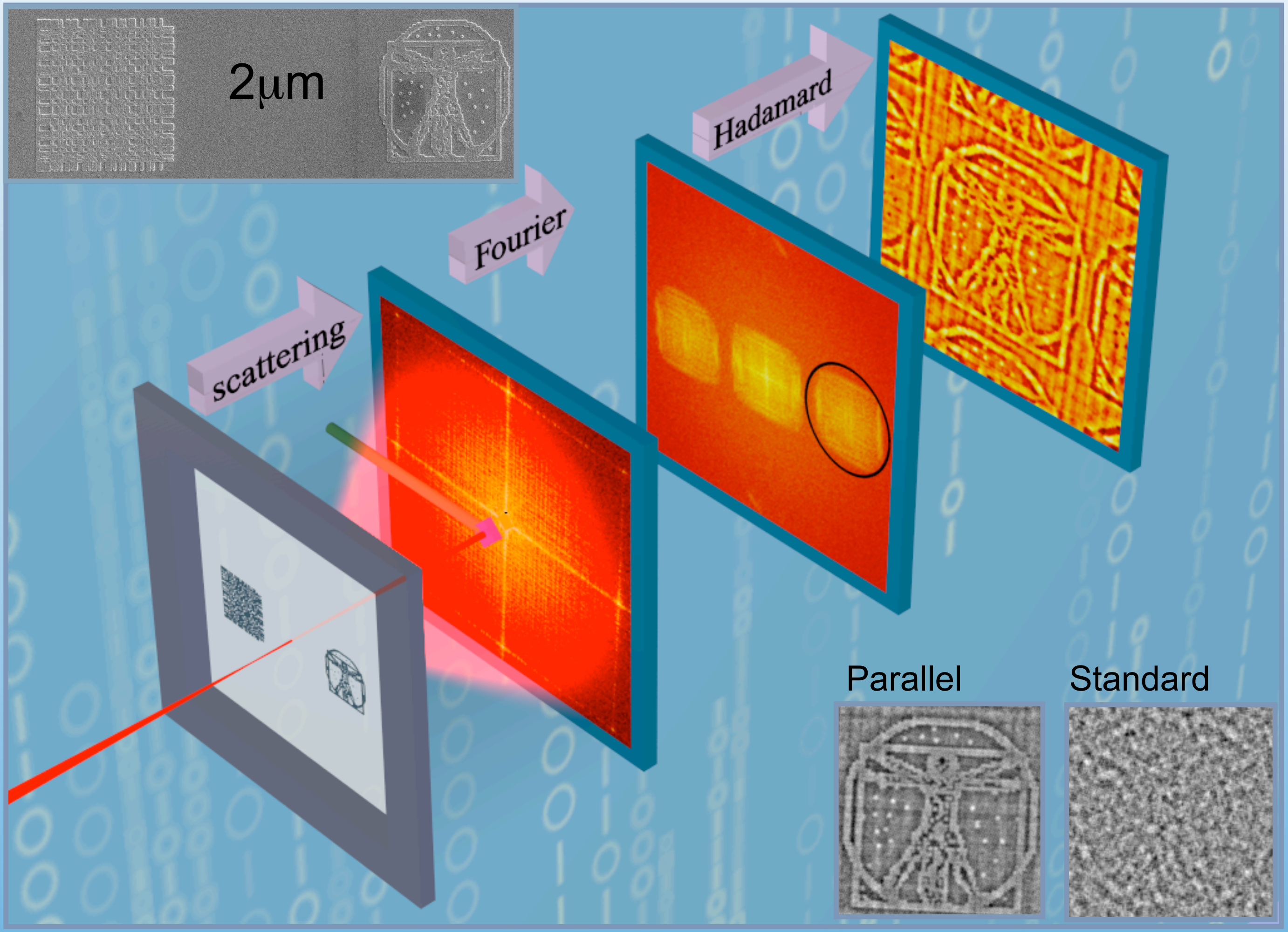

We improved the efficiency of holography by a factor of 2500

Signal to noise improvement

S. Marchesini et al. submitted

Fourier Transform Holography

The Fourier transform of the diffraction pattern provides the autocorrelation of the object, and a reference point generates a hologram in the autocorrelation map

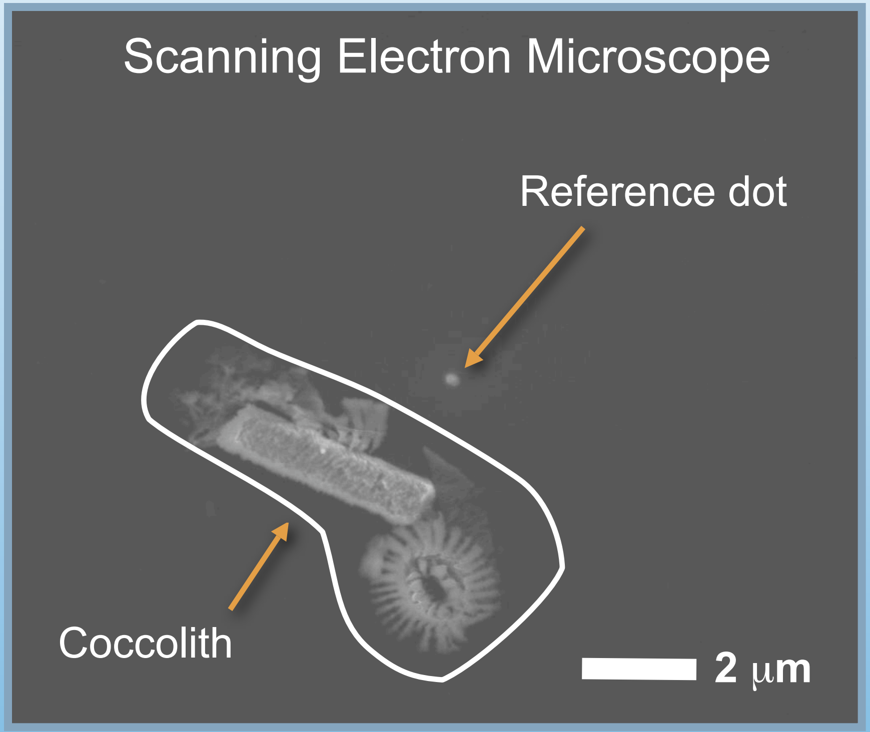

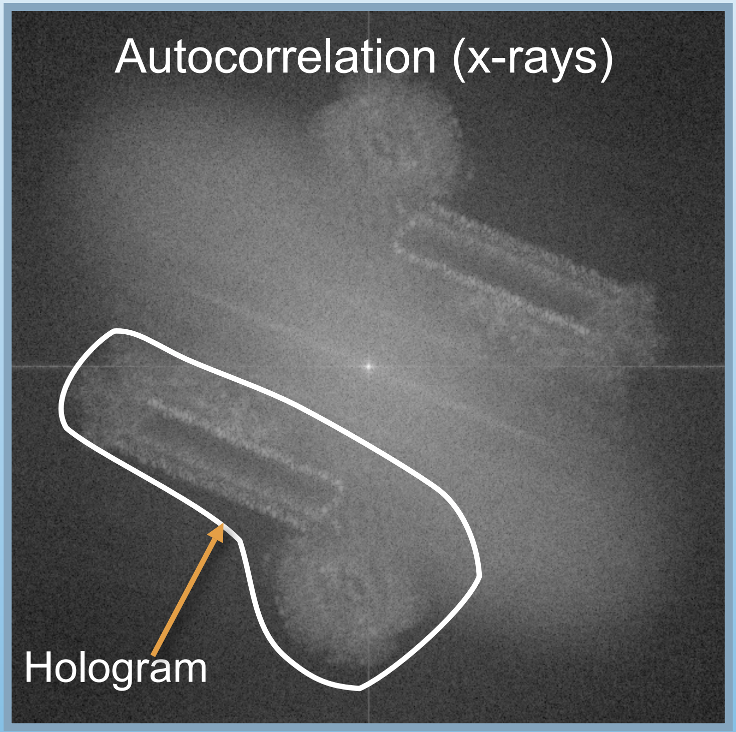

- The smaller the dot, the higher the resolution
- But the smaller the dot, the dimmer the hologram

Marchesini et al. IPAP CS 7, 380 (2006)

Coded Apertures Overcome Resolution Vs Brightness Limitations

One point creates a hologram, many points create overlapping holograms:
Like a pinhole camera with many pinholes.

The “magic trick”:
An extended object with point-like autocorrelation (uniformly redundant array)

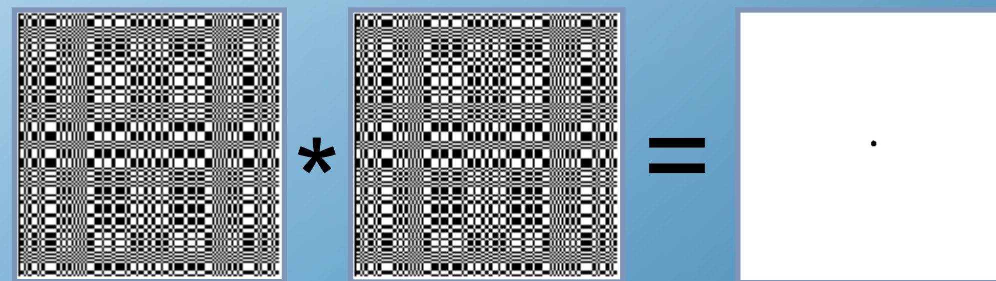

Coded apertures are used in many applications
Where lenses do not exist to improve signal

Pinhole camera

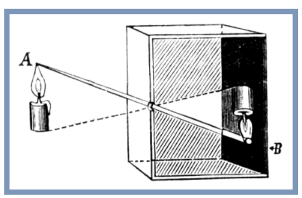

γ-ray astronomy

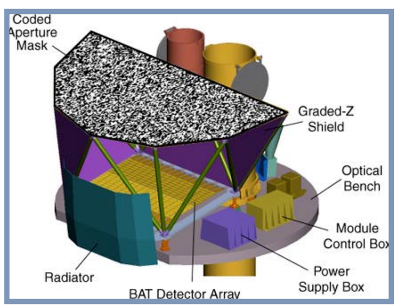

Medical imaging

Homeland security

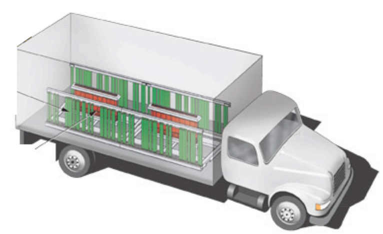

spectroscopy

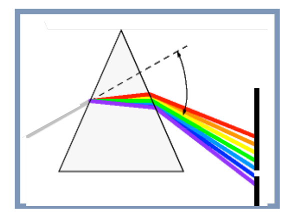

Ultrafast, Ultrabright, Ultra High Resolution X-ray Holography With Coded Apertures

λ=2.2 nm Resolution=43 nm, SNR X ~20

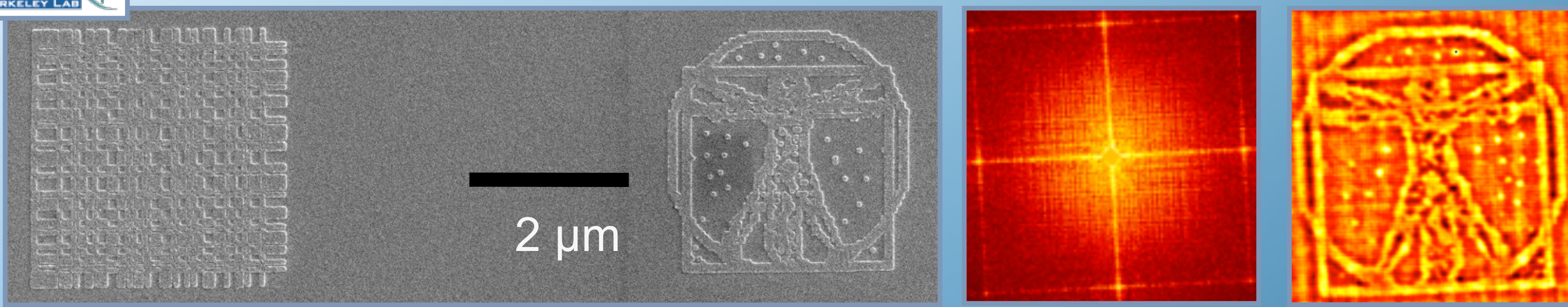

Δt=10 fs, λ=13.5 nm, Res~100 nm

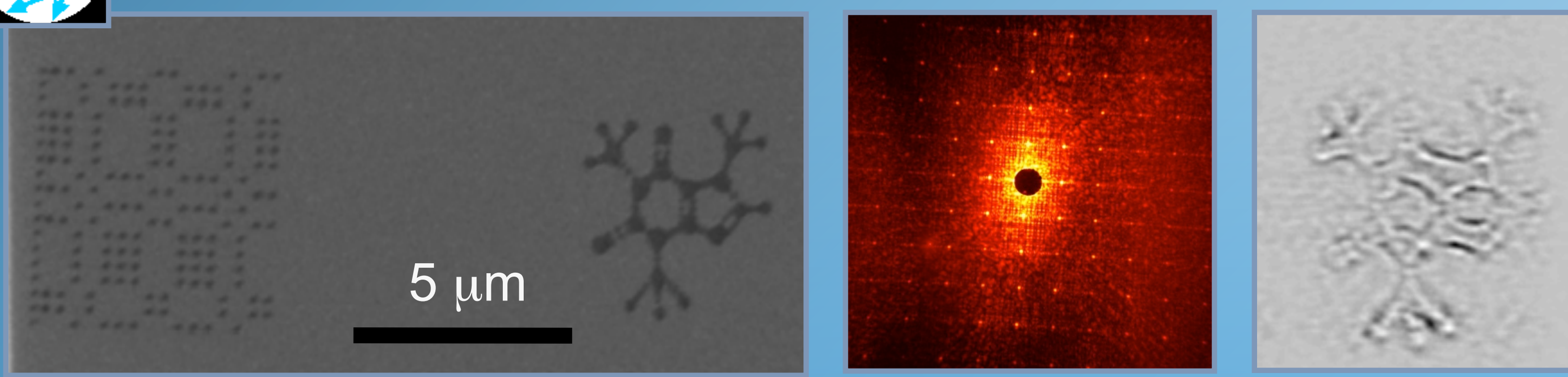

Sample from A. Sakdinawat

Overview Slide: Femtosecond Time Delay Holography

Motivation: to study the ultrafast dynamics of particles under intense x-ray fields

Scattering from a dusty mirror corroborates Livermore code for plasma dynamics

Scattering of 97 nm spheres ALS

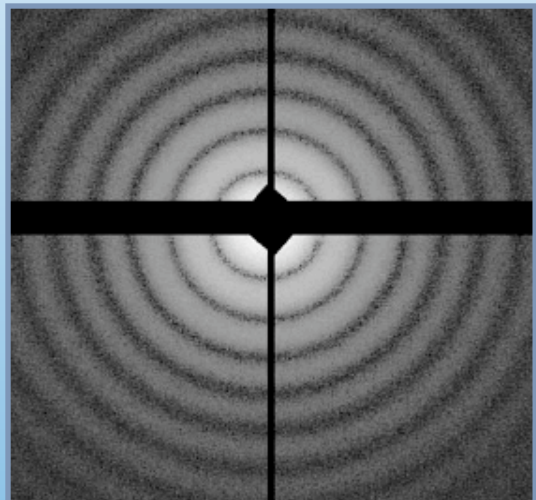

Size selection measured at ALS

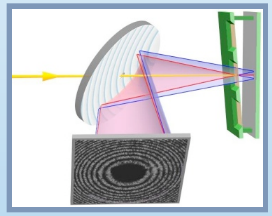

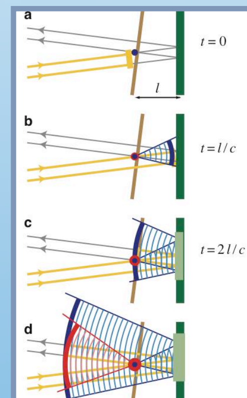

Time delay holography, FLASH

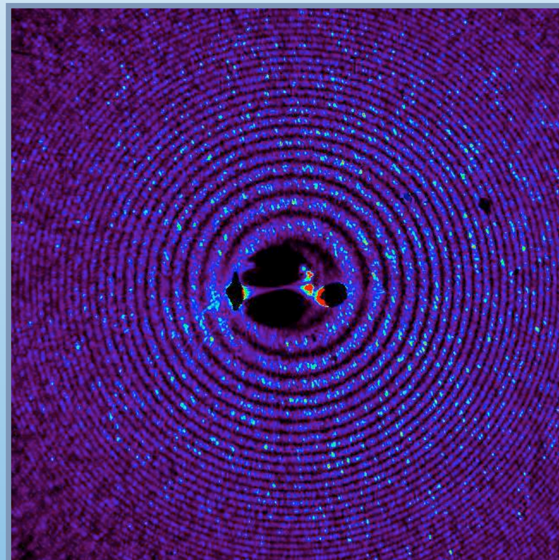

Density (g/cm^3)

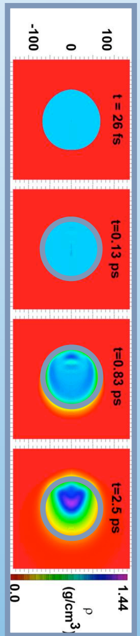

Plasma dynamics measured at FLASH

Successful experiments at the ALS have validated sample purification strategy and provided insight into data FLASH FEL expts.

Chapman et al. *Nature* 448, 676-679 (2007).

Mechanism of X-ray Induced Damage

Motivation: To study the ultrafast dynamics of particles under intense x-ray fields

Ionization leads to charge redistribution and explosion

- Some high-energy electron escape the molecule and charge it positively
- Remaining free electrons equilibrate and redistribute

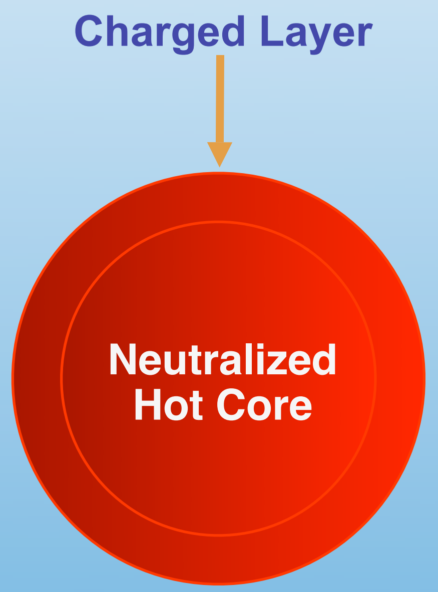

Trapped electrons shield the core, forming a 2-layer configuration

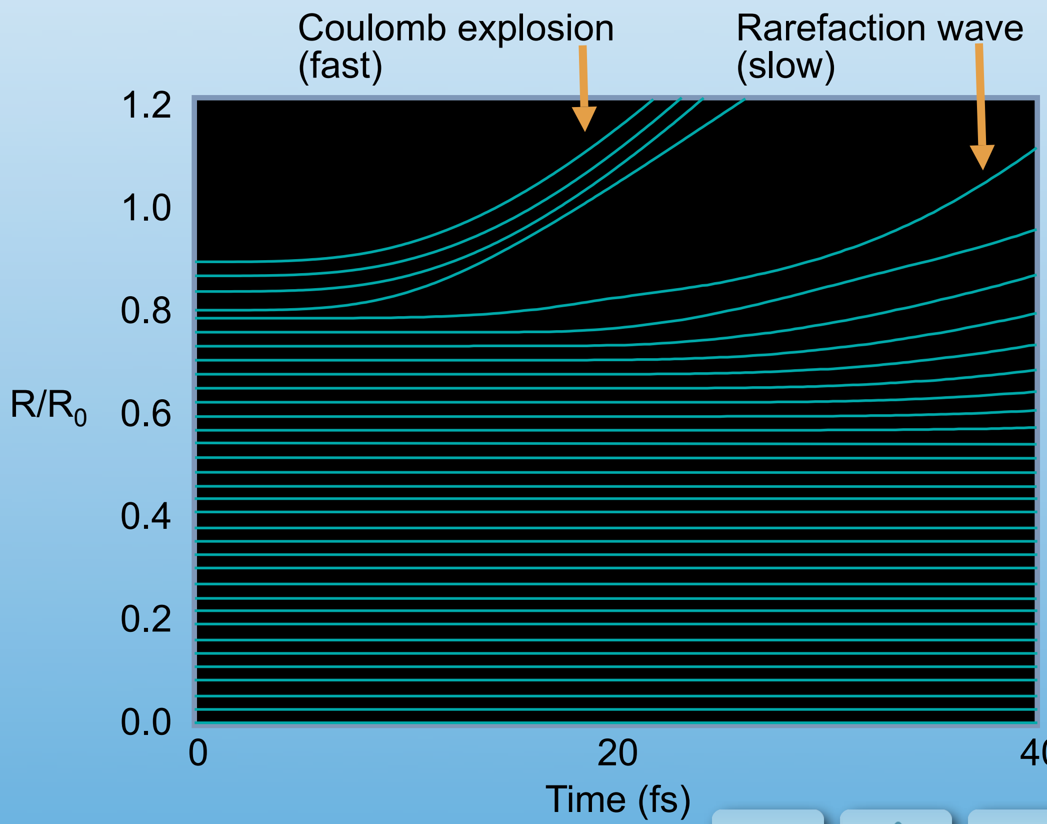

Selecting Identical Particles

Gas phase mobility separation for preparing size-monodisperse polystyrene nanoparticles

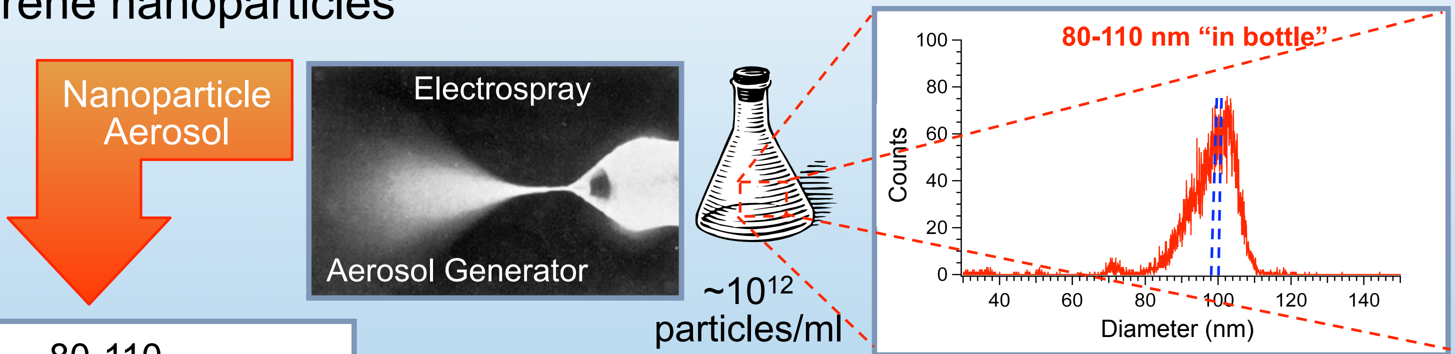

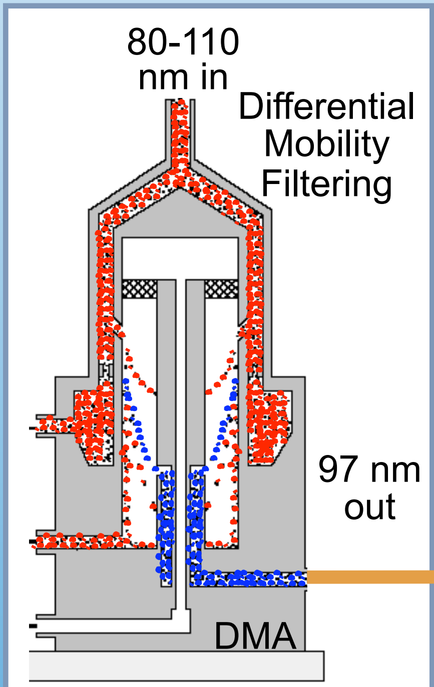

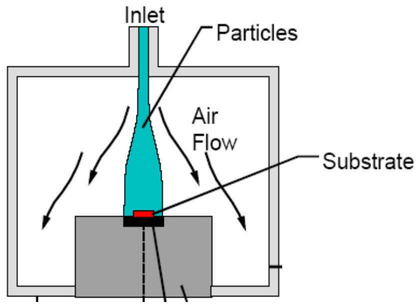

Nanometer Aerosol Sampler:

- Collects size-selected nanoparticles onto silicon nitride window

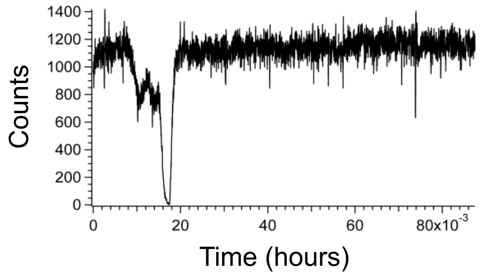

Monitor Aerosol Particle Number Density over time

- Condensation particle counter (CPC), light scattering

Mike Bogan, Henry Benner, Matthias Frank

Polystyrene Sphere Scattering Measured at the Advanced Light Source Validated <5% Size Variation

Successful experiments at the ALS have validated sample purification strategy and provided insight into data expected at upcoming VUV-FEL expts

Scattering of 97 nm spheres

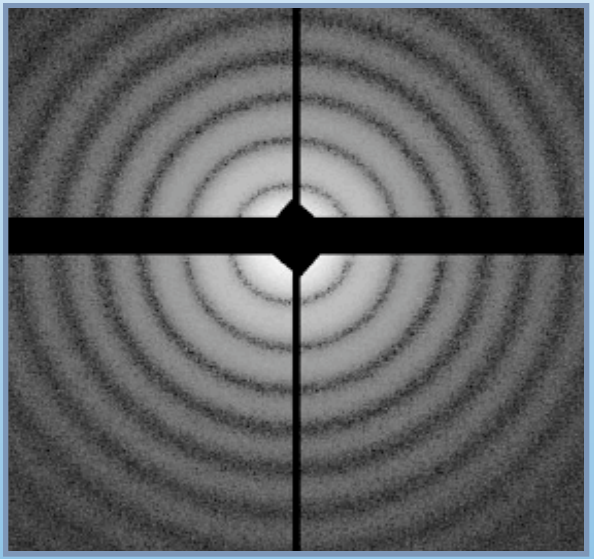

Wavelength = 1.65 nm
See 7th minima distinctly

Line-out Average of Diffraction Patterns

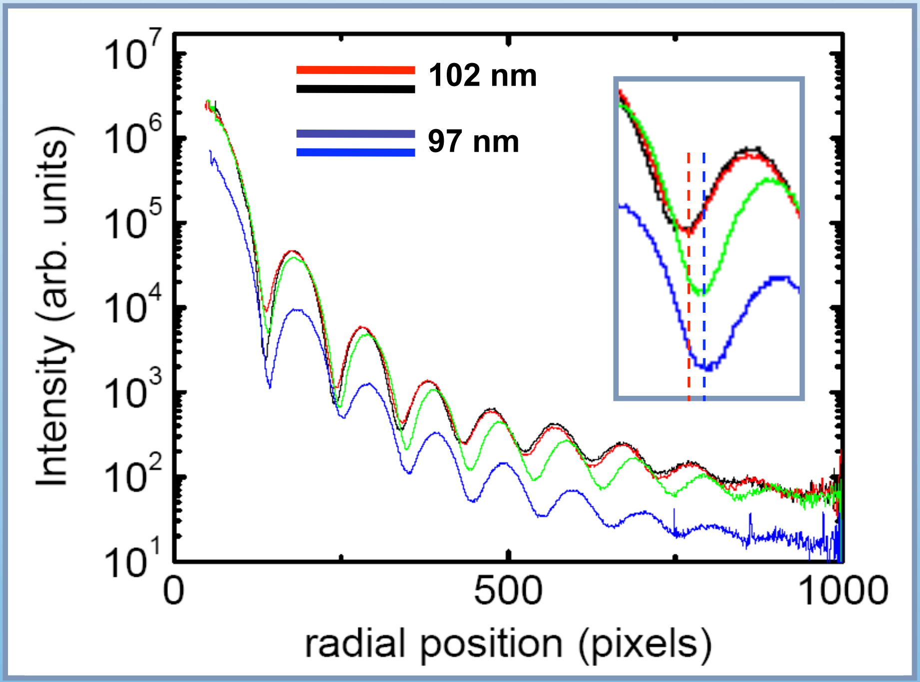

Easily differentiate particles with D = 97 and 102 nm, model shows <3.5% variation

Particle Explosion Experiments Were Performed at FLASH on Latex Particles on Membranes

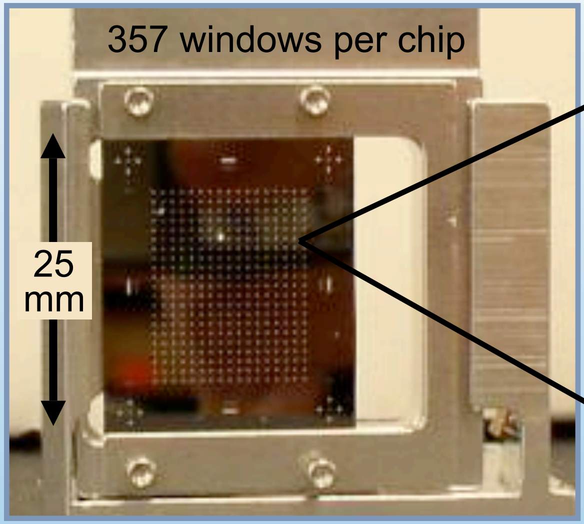

Mounted on piezo x-y stage to move each window into beam

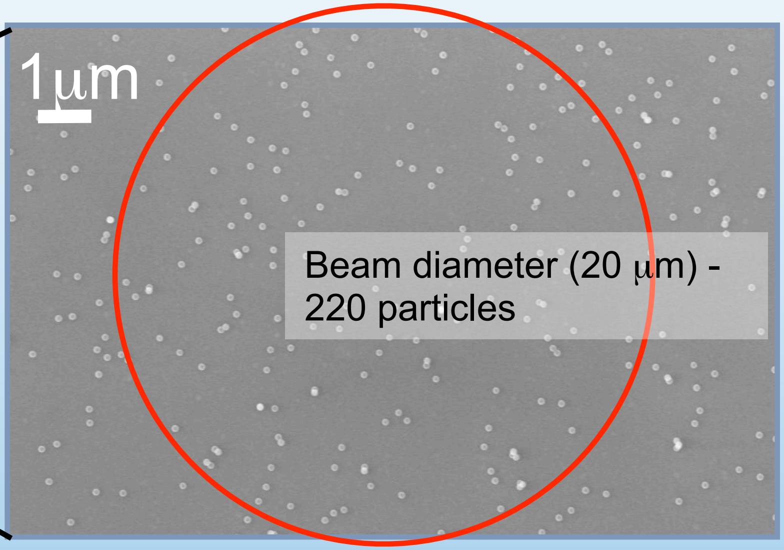

Latex particles on membrane

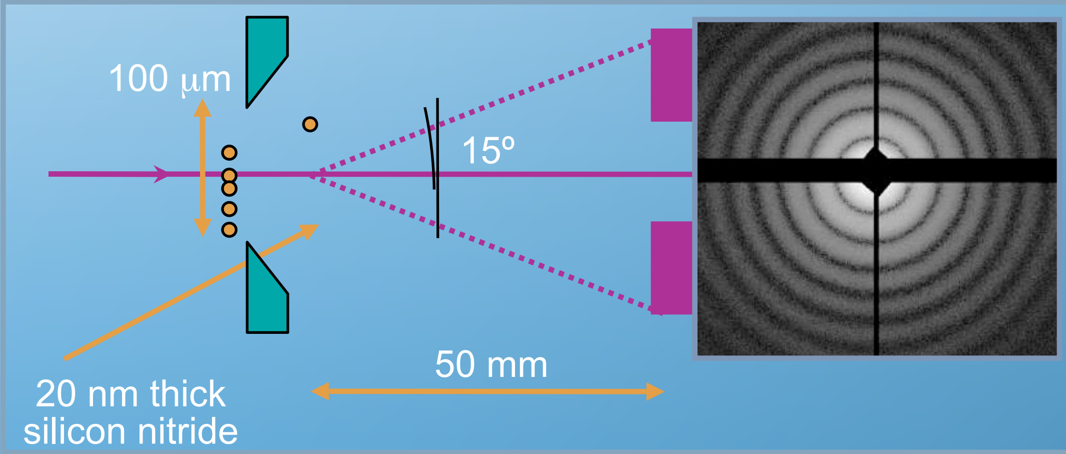

The particle size uniformity is determined by scattering at ALS

LLNL VUV Hydrodynamic Code Shows That Latex Spheres Start Exploding in ~ 2 Ps

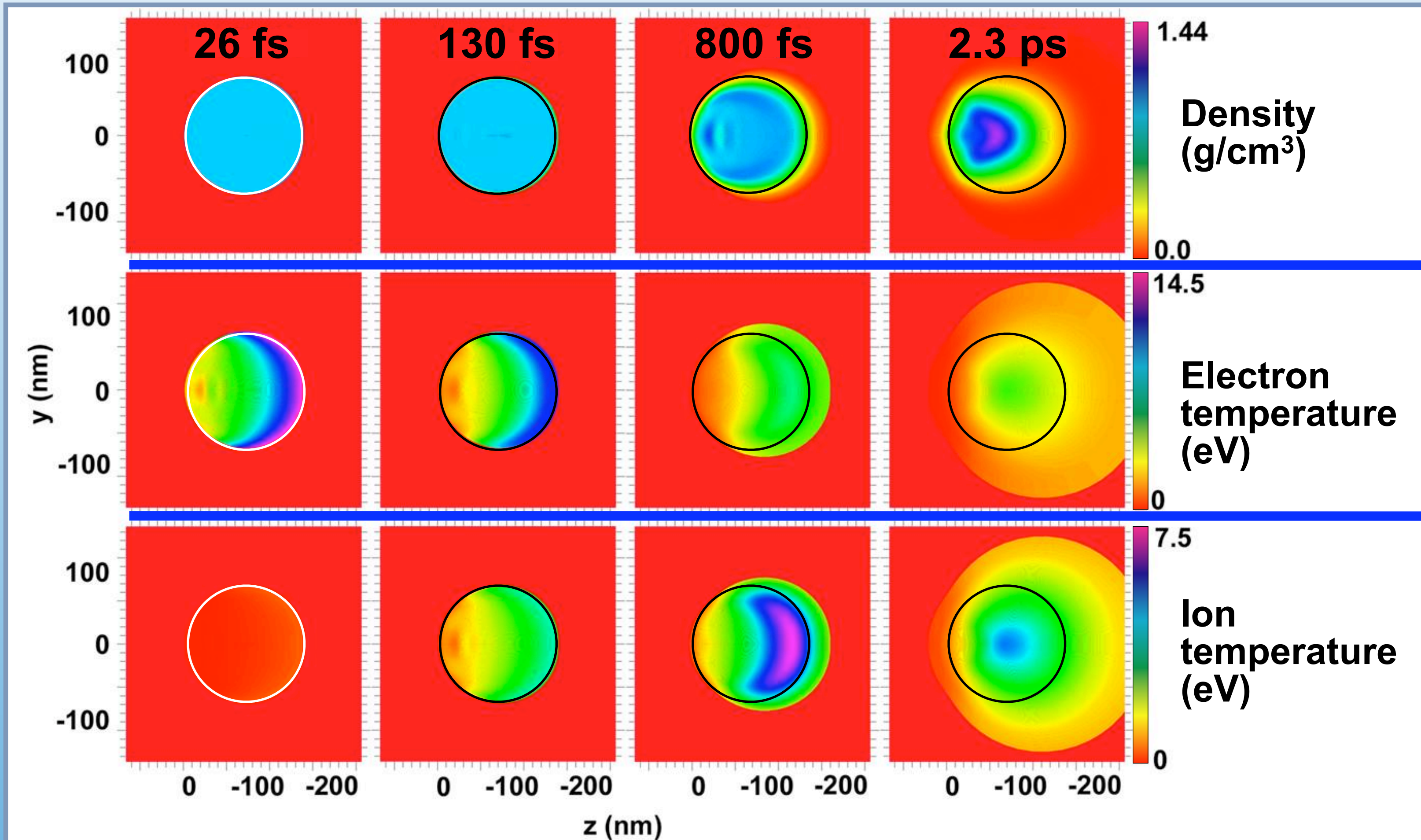

S. Hau-Riege et al., submitted

Scattering From Balls Demonstrates That They Retain Their Shape Throughout the Duration of the Pulse

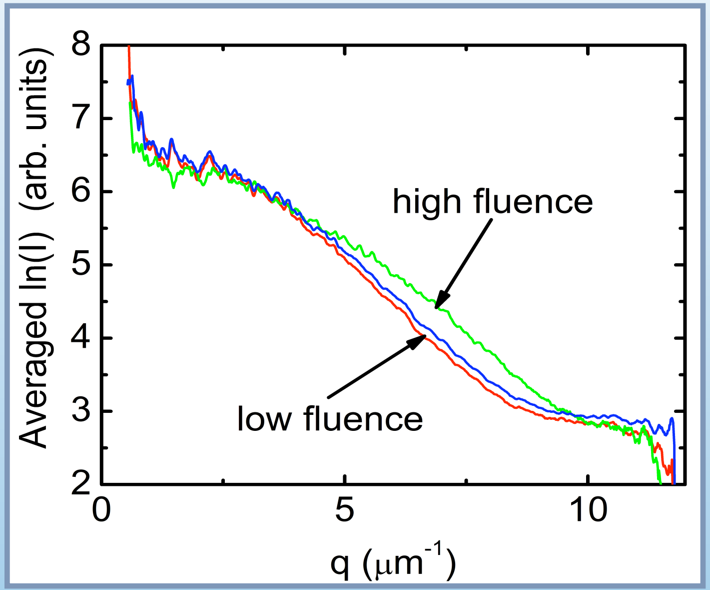

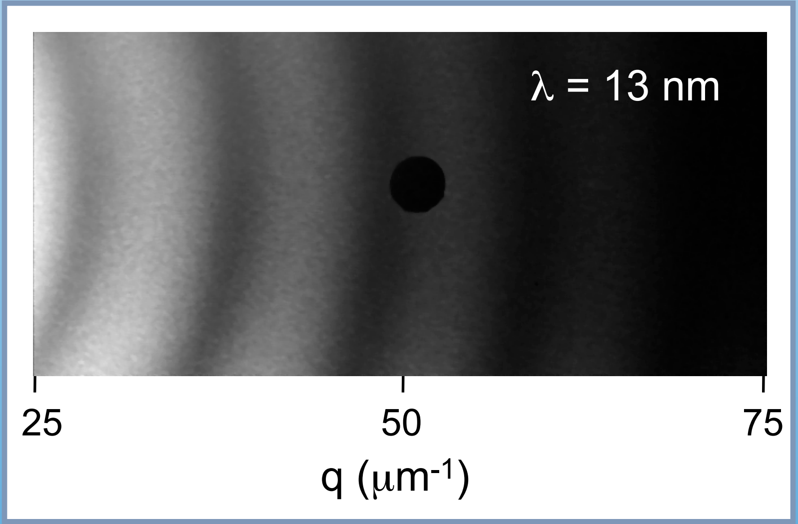

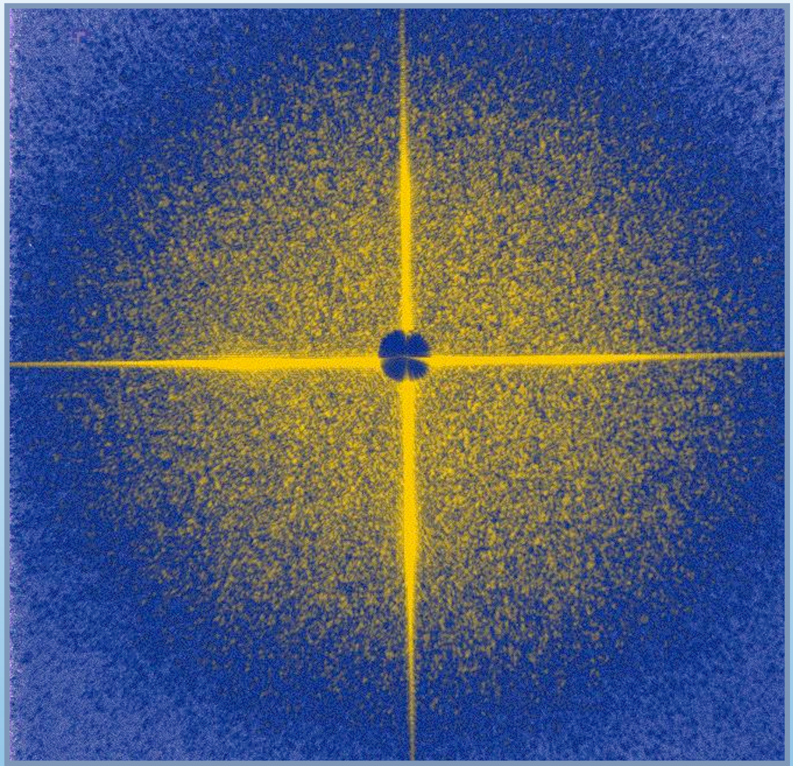

λ = 32 nm

We Applied Femtosecond Time-delay Holography to Study Explosion Process

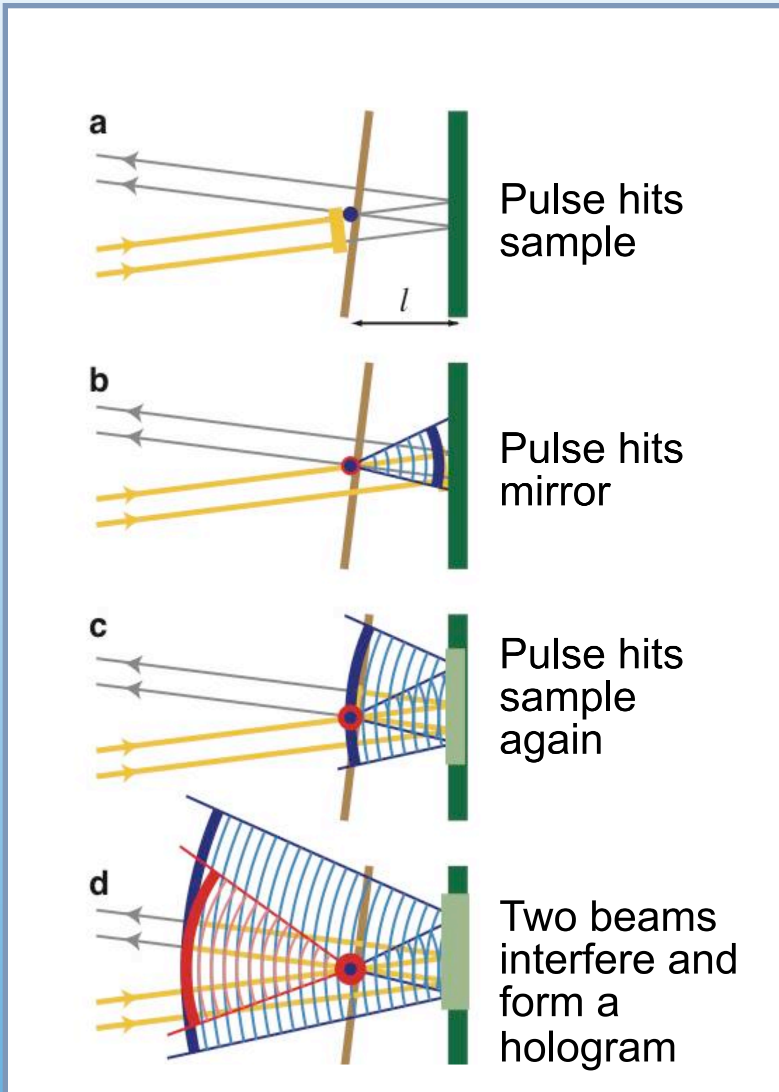

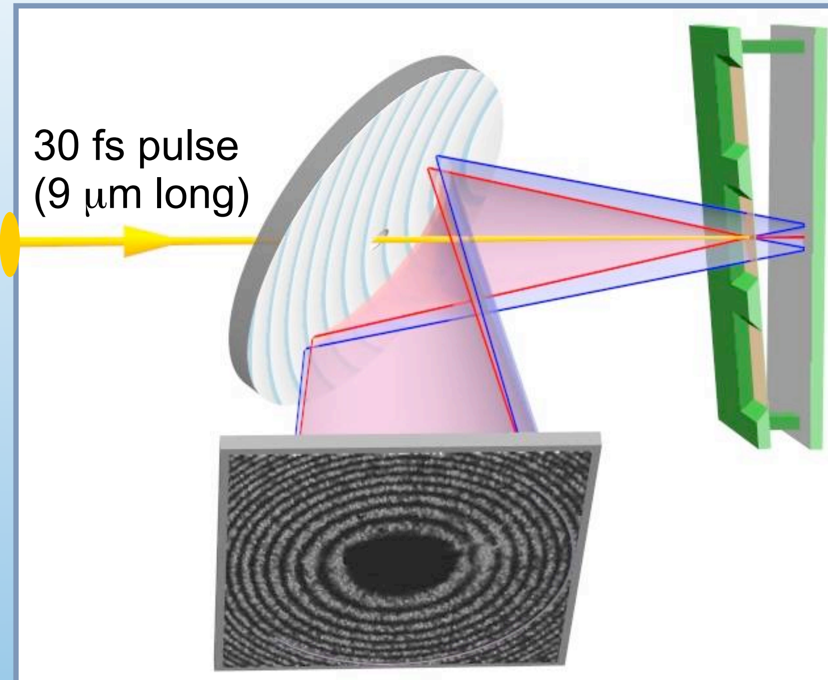

The hologram is reflected onto an area detector

Prompt diffraction

Delayed diffraction

Time delay 2 l / c

First Demonstration of Time-delay Holography With 3 Fs Time Resolution Indicates the Particle Explosion

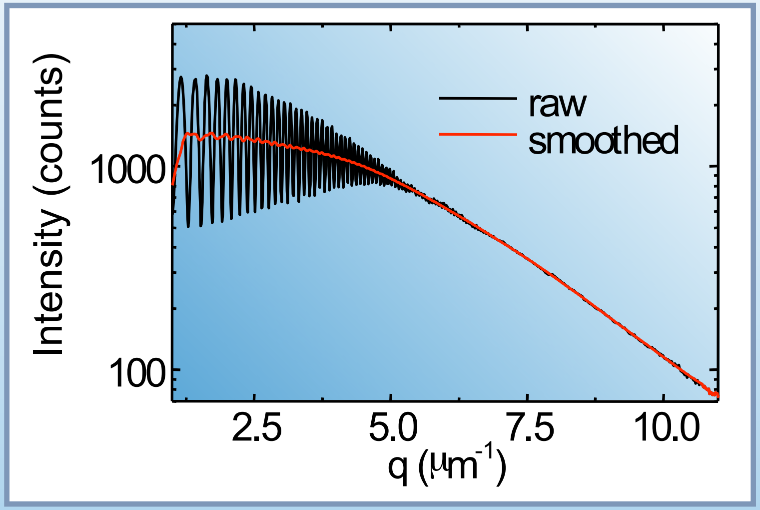

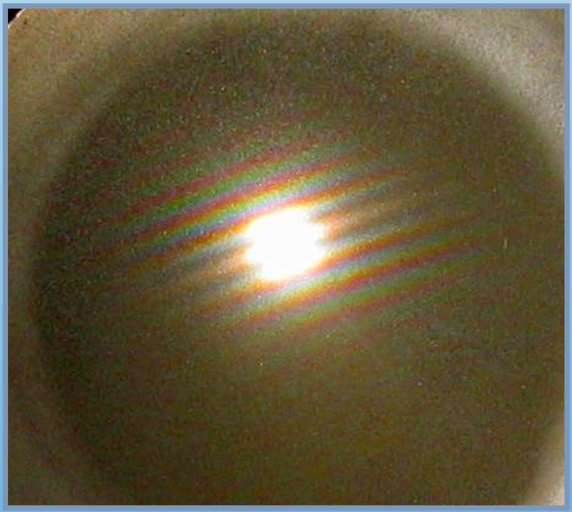

The “dusty mirror” experiment

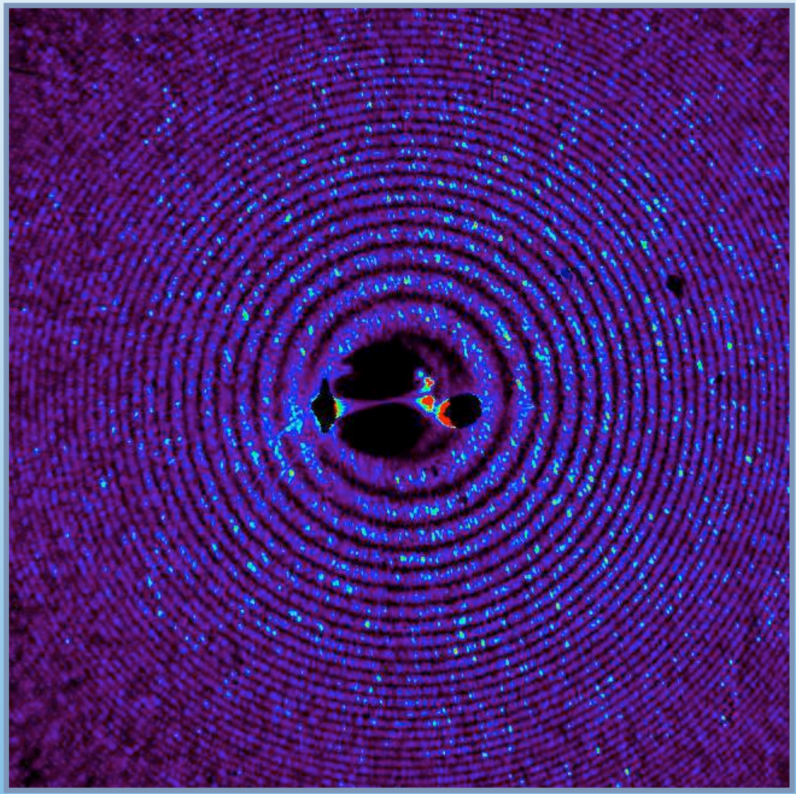

Single shot ultrafast time-delay X-ray hologram, with 300 fs delay

The Explosion Is in Good Agreement With Our Hydrodynamic Model

Experiments

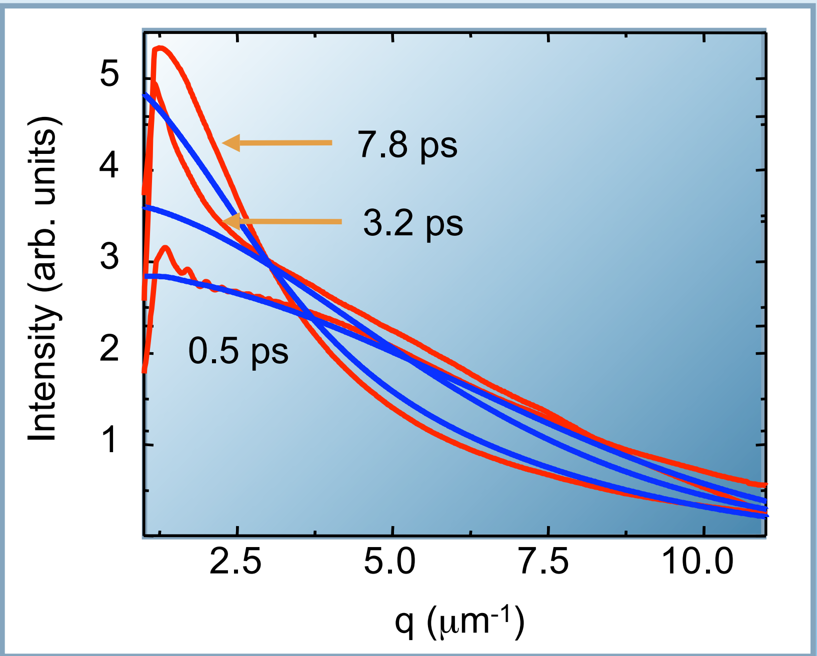

Calculation

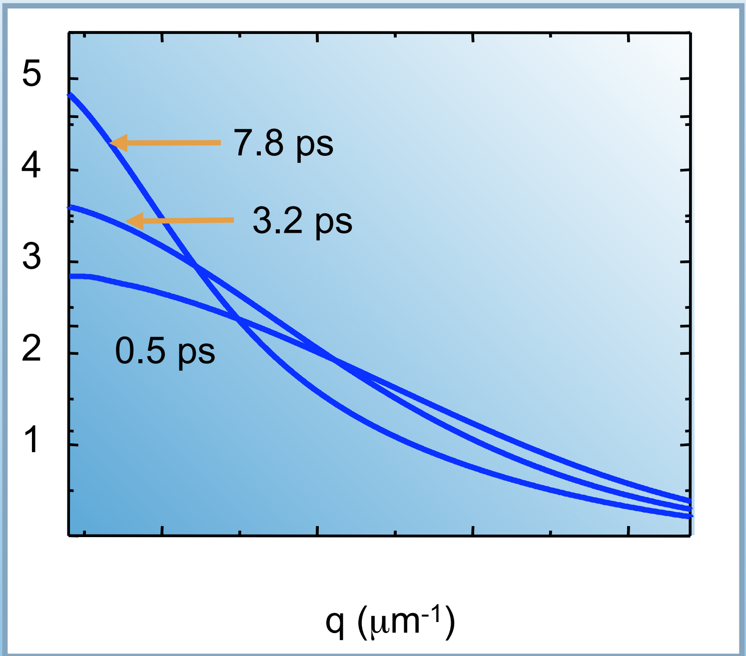

- The structure factor narrows, showing the particle exploding
- The lower resolution shape of the explosion is different than expected
- This is the first high-resolution observation of particle explosions

We Interferometrically Measure the Change in Optical Density of the Particle at Short Delays

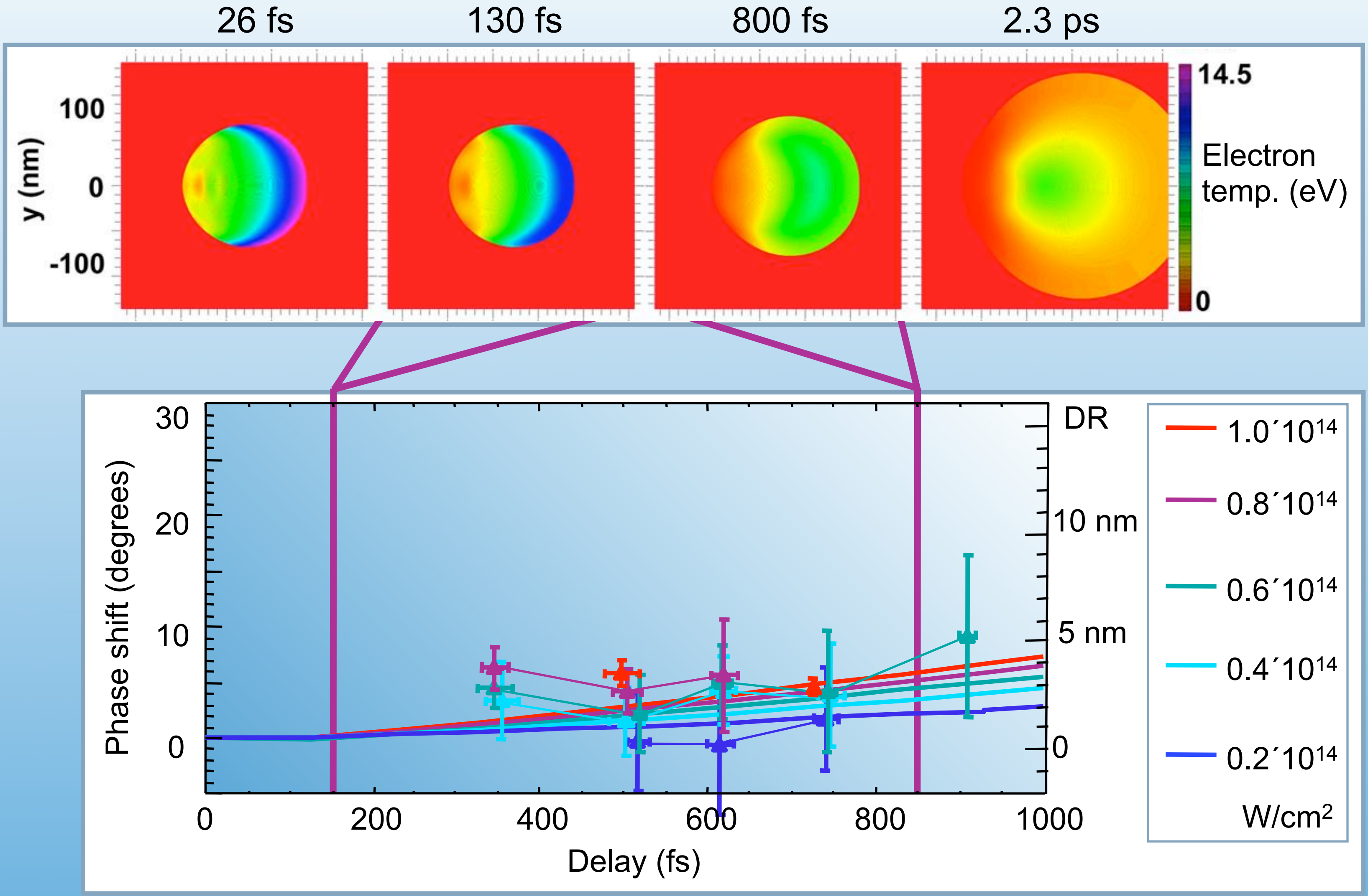

Injection Strategies for Imaging in Vacuo

Charge-reduced electrospray of nanoparticles

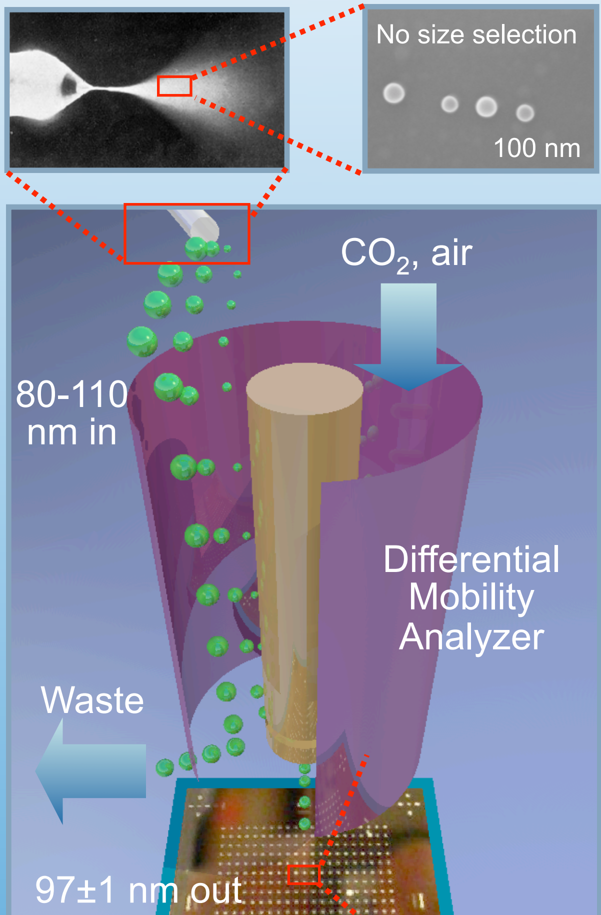

Calculated particle trajectories

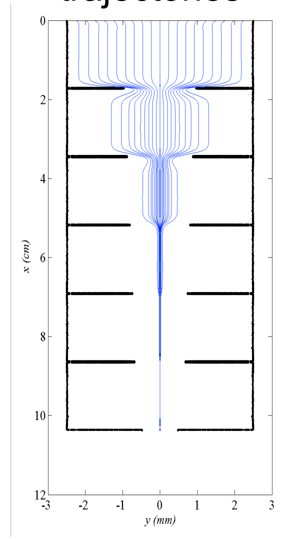

Injection system successfully used with FELs

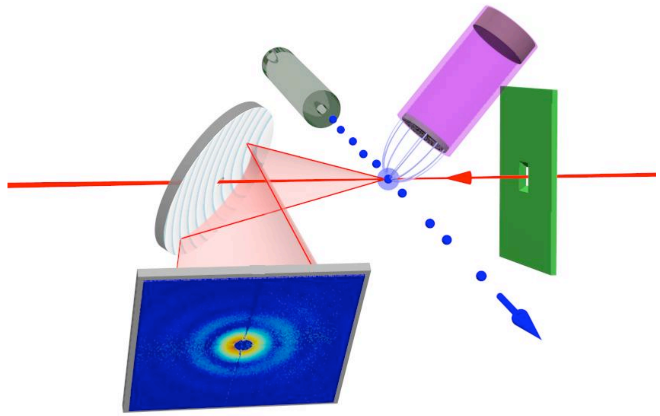

Mike Bogan, et al. Nanoletters, in press

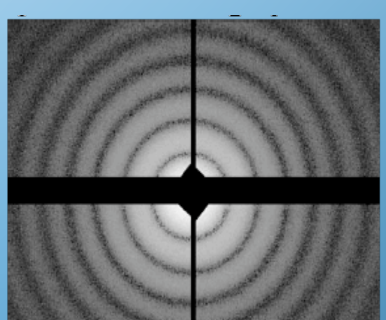

Validated Size selection

Triggered Aerojet injection tested at ALS

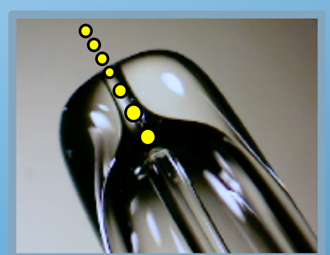

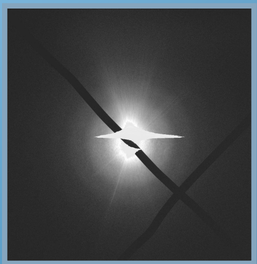

Weierstall, et al. NIM A in press

Serial Crystallography: Laser Alignment of Proteins

Motivation: To Image Proteins That Can't Be Crystallized

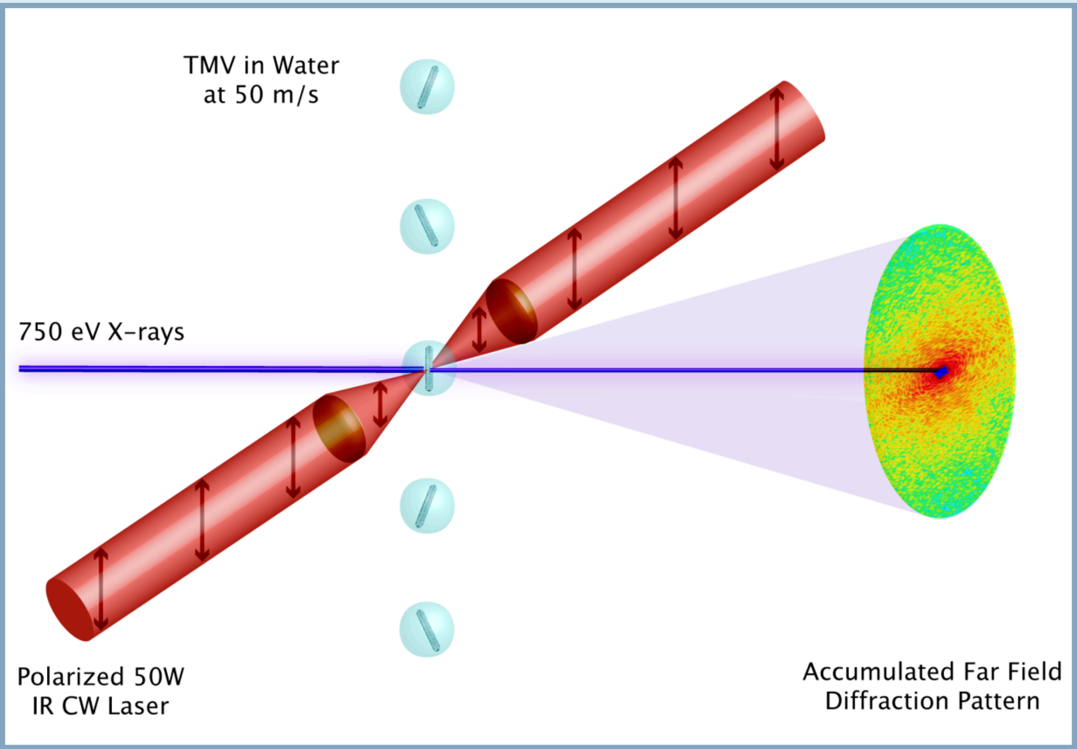

- Protein-in-water droplets injected into vacuum and rapidly cool by evaporation to form vitreous ice
- A polarized laser beam aligns the protein due to induced polarizability of the molecule
- X-ray diffraction is accumulated for many thousands of molecules
- When enough signal is accrued, polarization is rotated and diffraction recorded at a different angle
- 3D molecule image is obtained by phase retrieval (lensless imaging)

If alignment is good, one could use a standard synchrotron:

- Aligned molecules briefly pass through X-ray beam (exposure less than damage threshold)

J.C.H. Spence and R.B. Doak,
Phys. Rev. Lett. **92**, 198102 (2004)
J.C.H. Spence et al., Acta Cryst. A **61**, 237 (2005)

Diffraction rings

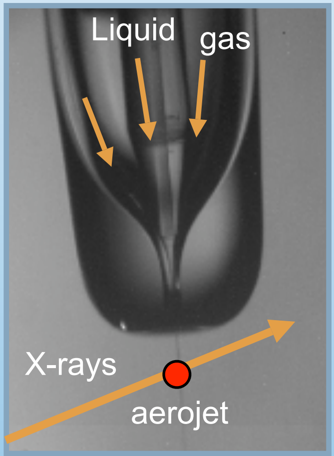

Weierstall et al. NIM A in press.

Worlds smallest protein nanocrystals (Photosystem 1)

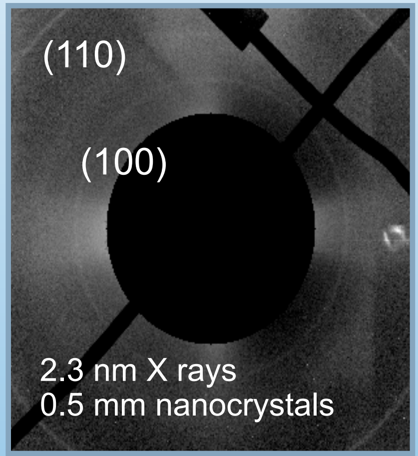

Shapiro et al summer 07 ALS 9.0.1

Laser alignment of injected proteins

To solve proteins which can't be crystallized.
Method: Spray proteins, align by laser and image.

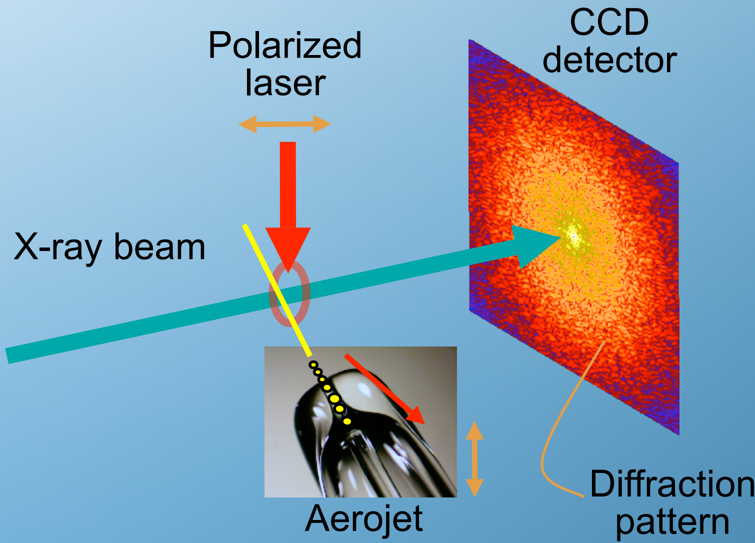

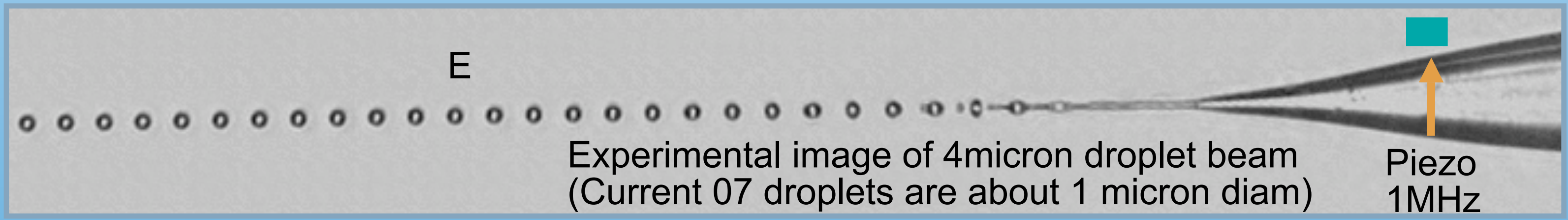

Experimental image of 4micron droplet beam
(Current 07 droplets are about 1 micron diam)

*Spence, Doak, Weierstall, Starodub, DePonte, Schmidt, Fromme,Hembree. ASU NSF IDBR $.
*Chapman, Spence, Howells, Shapiro, Weierstall, Doak. ALS, ASU XRD CBST $

Computational Lenses

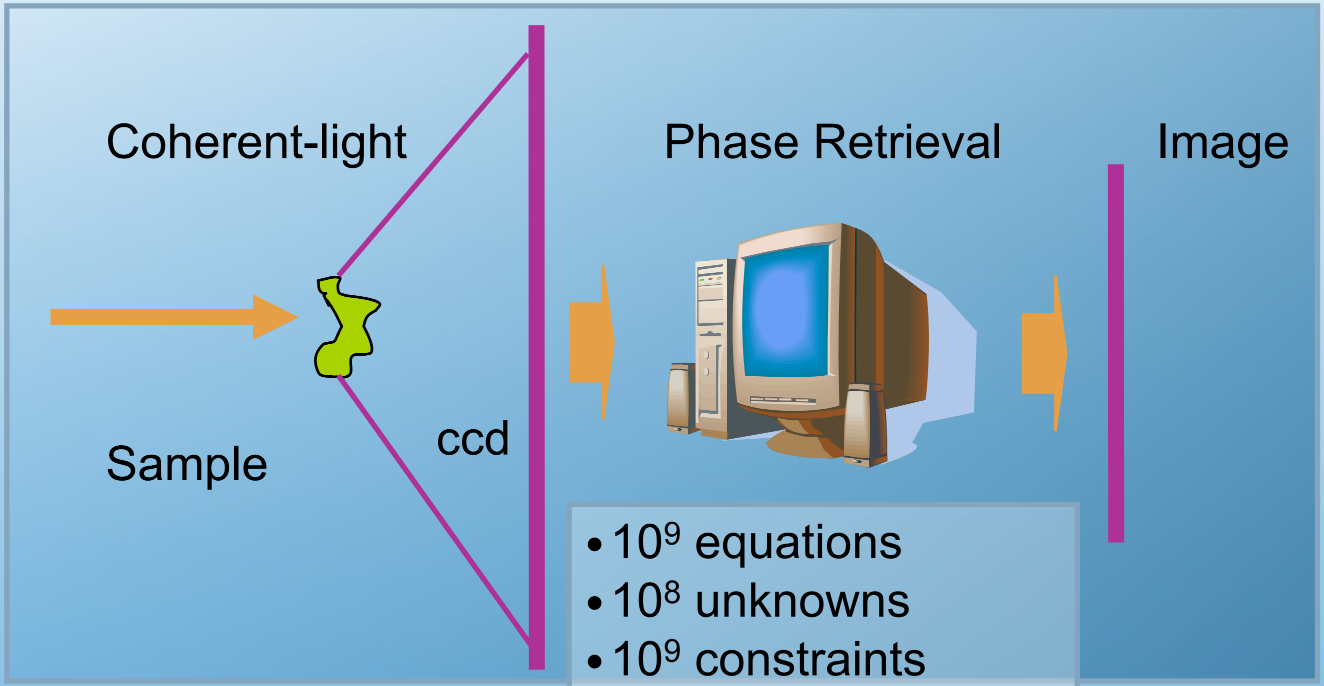

- 10^9 equations
- 10^8 unknowns
- 10^9 constraints

Large-scale, non-linear, non-convex, non-smooth

ALS organized the first and last of a series of international conferences on coherent x-ray imaging

We are leading the development of reconstruction methods

Shrinkwrap algorithm, S. Marchesini et al, Phys Rev B 68, 140101(R) (2003).
Hybrid input output with quasi-Newton optimization, S. Marchesini et al. Rev. Sci. Inst. 78, 011301 (2007)

We Improved the Speed and Reliability of Reconstruction Methods

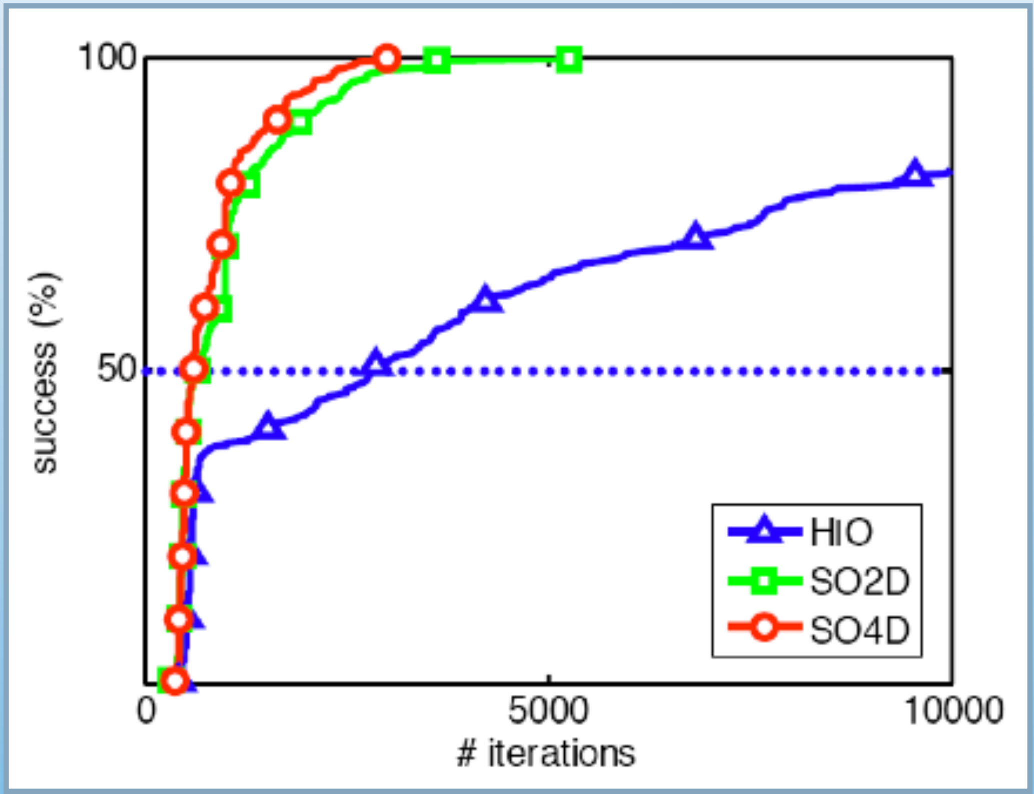

Complex Lena

2D Step size optimization
4D Step size optimization

S. Marchesini, JOSA A 24, 3289-3296

Collaborations

LBNL: Malcolm Howells, Janos Kirz, David Shapiro, Stefano Marchesini

Stony Brook: Xiaojing Huang, Chris Jacobsen, Janos Kirz, Enju Lima Huijie Miao Aaron M. Neiman, Johanna Nelson, David Sayre, Jan Steinbrener, Andrew Stewart

SLAC: Sebastien Boutet

LLNL: Anton Barty, Henry Chapman, Stefan Hau-Riege,

ASU: John Spence, Uwe Weierstall, Bruce Doak, Dan Deponte